Chapter 2
Lithium Batteries

2.1 Introduction

By placing a very pure lithium-metal foil as anode element and a lithium salt in a nonaqueous solution as electrolyte, a new generation of electrochemical generators was born in the mid-1960s. Basically, the charge transport is identical to nickel-metal hydride (Ni-MH) or nickel-cadmium (Ni-Cd) batteries, except that Li^+ ions are created by the simple reaction

$$Li \rightarrow Li^+ + e^-, \tag{2.1}$$

liberating one electron through the external circuit and one ion introduced into the porous structure of the cathode. As discussed in the first chapter, the main parameters of energy storage systems are energy density (gravimetric and volumetric), power density, energy efficiency, and energy quality [1]. The great attractiveness of the lithium technology comes from the fact that Li is a lighter metal (molar weight $M_w = 6.941$ g mol^{-1} and density 0.51 g cm^{-3}), with the electronic configuration $(He)2s^1$. The specific capacity of Li metal is 3860 mAh g^{-1} and the couple Li^0 has the highest electroactivity with standard redox potential -3.04 V against H_2/H^+. Consequently, the voltage of lithium batteries is also significantly higher than that of the Pb-acid and Ni-metal hydride, because lithium is the most electropositive element found in nature.

Primary and secondary lithium batteries using a nonaqueous electrolyte, exhibit higher energy density than aqueous electrolyte-based batteries due to the cell potential higher than 1.23 V, the thermodynamic limitation of water at 25 °C. The excellent performances of nonaqueous lithium batteries may meet the need for high power batteries in micro-devices, portable equipment, and even electrical vehicles.

Lithium does not exist in the form of pure metal in nature due to a very high reactivity with air, nitrogen and water. It is extracted from ore or brine salt marsh

C. Julien et al., *Lithium Batteries*, DOI 10.1007/978-3-319-19108-9_2

(lithium chloride LiCl, lithium hydroxide LiOH, lithium carbonate Li_2CO_3). Since we only have 112.7 g of lithium in one kilo of Li_2CO_3, the extraction of one kilogram of lithium requires 5.3 kg of lithium carbonate. According to the US Geological survey (January 2010), Bolivia would house 32 % of world reserves of lithium carbonate (Li_2CO_3), and Chile nearly 27 %. However, Chile, China, and Argentina are the largest producers [2]. Note that 0.8 kg of lithium metal is produced per second in the world that is 25000 tons a year, mainly to produce lithium-ion batteries for electric cars or cell phones. In the US Geologican survey, Goonan said that it would take 1.4–3.0 kg of lithium equivalent (7.5–16.0 kg of lithium carbonate) to support a 40-mile trip in an electric vehicle before requiring recharge [2].

In this chapter, attention is focused on the technology of the lithium batteries. After a brief historical overview, we draw most of the primary and secondary lithium batteries. To get further information on the interest of these power sources, we invite the readers to consult works in references as there have been published numerous excellent books on LiBs based on various different viewpoints [3–16]. However, there are few books available on the state-of-the-art and future of next generation LiBs, particularly eventually for EVs and HEVs.

2.2 Historical Overview

Research in lithium batteries began in 1912 under G.N. Lewis, but the breakthrough came in 1958 when Harris noticed the stability of Li-metal in a number of nonaqueous (aprotic) electrolytes such as fused salts, liquid SO_2, or lithium salt into an organic solvent such as $LiClO_4$ in propylene carbonate ($C_4H_6O_3$). The formation of a passivation layer that prevents the direct chemical reaction between lithium metal and the electrolyte but still allows for ionic transport is at the origin of the stability of lithium batteries [17].

These researches opened the door to the fabrication and commercialization of varieties of primary lithium batteries; since the late 1960s nonaqueous lithium cells, especially the 3-V primary systems, have been developed. These systems include lithium-sulfur dioxide (Li//SO_2) cells, lithium-polycarbon monofluoride (Li//$(CF_x)_n$) cells introduced by Matsuschita in 1973, lithium-manganese oxide (Li//MnO_2) cells commercialized by Sanyo in 1975, lithium-copper oxide (Li//CuO) cells, lithium-iodine (Li//$(P2VP)I_n$) cells. During the same period, molten salt systems (LiCl-KCl eutecticum) using a Li-Al alloy anode and a FeS cathode were introduced [1]. The lithium-iodine battery has been used to power more than four million cardiac pacemakers since its introduction in 1972. During this time the lithium-iodine system has established a record of reliability and performance unsurpassed by any other electrochemical power source [18].

In the early 1970s was discovered the reversible insertion of guest species (ions, organic molecules, organometallics) into an host lattice that maintains its structural features but exhibits new physical properties. The first work was initiated by

Table 2.1 Rechargeable lithium metal batteries using TM oxides as positive electrodes

Battery	Potential (V)	Specific energy (Wh kg^{-1})	Company/year
Li//V_2O_5	1.5	10	Toshiba 1989
Li//CDMO[a]	3.0	–	Sanyo 1989
Li//$Li_{0.33}MnO_2$	3.0	50	Taridan 1989
Li/VO_x	3.2	200	Hydro-Québec 1990

[a]Composite dimensional manganese dioxide

Armand at Stanford [19] on the properties of Prussian blue (iron cyanide bronzes $M_{0.5}Fe(CN)_3$). Among a great variety of inorganic materials, transition-metal oxide (TMOs) as CrO_3 was investigated by Armand at Grenoble [20] and transition-metal dichalcogenides (TMDs) were studied by DiSalvo at Bell Laboratories [21], and later by researchers at EXXON [22–25]. Rechargeable lithium cells using Li-insertion compounds as positive electrodes were developed in the mid 1970s, when Winn and Steele [26, 27] at Chloride Technical Ltd reported solid-solution electrode of TiS_2 with lithium and sodium as well, followed by the announcement of Exxon (USA) for its intention to commercialize the Li//TiS_2 system [28]; Bell Laboratories (USA) reported the development of lithium cells constructed with either $NbSe_3$ or TiS_3 [29], while transition-metal oxides such as V_2O_5, V_6O_{13} were investigated by Dickens in the UK [30]. Table 2.1 documents the numerous efforts toward the development of rechargeable lithium batteries using TMOs as positive electrode and Li metal as anode.

Prototype cells using the principle of lithium intercalation showed promising characteristics of very high energy density (for instance, 3 times that of Ni-MH cells), moderate cycle life and higher voltage (~3 V) than aqueous technologies. Beside the development of positive electrodes, Li alloys (for instance, Li-Al) were envisaged as negative electrodes. Among them, the first commercially available rechargeable lithium power source system, the Li//MoS_2 type battery (MOLICEL™) was manufactured by Moli Energy Ltd. in Canada. This cell delivers performance with sustained drain rates of several amperes at a cell voltage between 2.3 and 1.3 V. The energy density was in the 60–65 Wh kg^{-1} range at a discharge rate of *C*/3 (approximately 800 mA). The total capacity of a *C*-size cell was 3.7 Ah and the number of realizable cycles is dependent upon the charge and discharge conditions [10]. Especially manufactured as the power source for pocket telephones in Japan, the first attempt to fabricate rechargeable batteries has proven very difficult ensuing safety concerns including fires due to the formation of dendrites. All the products were recalled [31].

At Eveready Battery Co. (USA) a Li/chalcogenide glass/TiS_2 was designed for the CMOS memory backup market. This cell is based on phosphorous chalcogenide glasses $Li_8P_4O_{0.25}S_{13.75}$ mixed with LiI and on solid-solution composite electrode TiS_2-solid electrolyte-black carbon with the percentage by weight of 51:42:7. The cathode capacity ranges from 1.0 to 9.5 mAh. The cell packaging is a standard sized XR2016 coin cell. The impedance of the cell at 21 °C is between 25 and 100 Ω depending upon where the cell is in the charge–discharge cycle. More than

200 cycles have been obtained in experimental cells [32]. A spirally wound AA-size Li//TiS_2 cell has been constructed by Grace Co. (USA). At 200 mA discharge rate, 1 Ah is delivered to 1.7 V [33]. In *C*-size, a Li//TiS_2 cell built by EIC Laboratories Inc. (USA), a capacity of 1.6 Ah was obtained. This cell operates in the temperature range from −20 to +20 °C [34].

The concept of lithium rocking-chair cells or lithium-ion batteries (LiBs) is not new. It has been proposed in the late 1970s by Armand who suggested *to use two different intercalation compounds as a positive and negative electrode, in the so-called rocking-chair battery, the lithium ions being transferred from one side to the other* [35]. Practically they were demonstrated in the early 1980s [36].

However, this concept has gained renewed attention following the success of Japanese industries. Sony and Sanyo in 1985 and 1988, respectively [37, 38], started to apply new electrodes materials following the fundamental researches of Goodenough in Oxford [39, 40] and of Armand and Touzain in Grenoble [41], who evidenced the fast motion of lithium ions in layered host structures (named as *lithium intercalation compounds*). A LiB contains a high-voltage (cathode) and a low voltage (anode) host versus Li^0/Li^+ redox couple. Exploiting the idea for large-scale production, Sony Energytec Inc. has commercialized in June 1991 a Li-ion battery including a lithium cobaltate ($LiCoO_2$) and a non-graphitic carbon (lithiated coke LiC_6), as cathode and anode, respectively; target was powering mobile phones. The Li-ion battery by Sony was an 18650-type (253 Wh L^{-1} energy density) using $LiPF_6$ in propylene carbonate/diethyl carbonate electrolyte solution [42]. Table 2.2 lists the initial applied patents for the invention of LiBs. The first patent related to the construction of a LiB, issued on 5 October 1985, is the property of the Japanese company Asahi Chemical Ind.

During the following decades, active R&D was directed towards alternative electrode materials resulting in small, light and high energy density batteries that have subsequently allowed the rapid development of small portable electronics.

Table 2.2 Prior patents related to Li-ion batteries

Inventor/company	Patent title	Patent number	Application date
Goodenough JB, Mizushima K (Kingdom Atomic Energy)	Fast ion conductors ($A_xM_yO_2$)	US 4,357,215 A	5 Avr 1979
Goodenough JB, Mizushima K (Kingdom Atomic Energy)	Electrochemical cell with new fast ion conductors	US 4,302,518	31 March 1980
Ikeda H, Narukawa K, Nakashima H (Sanyo)	Graphite/Li in nonaqueous solvents	Japan 1,769,661	18 June 1981
Basu S (Bell Labs)	Graphite/Li in nonaqueous solvents	US 4,423,125	13 Sept 1982
Yoshino A, Jitsuchika K, Nakajima T (Asahi Chemical Ind.)	Li-ion battery based on carbonaceous material	Japan 1,989,293	5 Oct 1985
Nishi N, Azuma H, Omaru A (Sony Corp.)	Non aqueous electrolyte cell	US 4,959,281	29 Aug 1989

Table 2.3 Energy densities at a *C*/5 discharge rate of some commercialized Li-ion batteries

Cell	Energy density	
	Gravimetric (Wh kg^{-1})	Volumetric (Wh dm^{-3})
Sony US 18650	103	245
A&T LSR 18650	130	321
Sanyo UR 18650	126	288
Moli ICR 18650	113	287
Matsushita CGR 17500	129	269
SAFT VL18650	108	260

Table 2.4 Chemistry of various primary lithium batteries. Reproduced with permission from [45]. Copyright 1997 CRC Press

Liquid electrolyte cells		Solid electrolyte cells
Solid cathode	Liquid cathode	Solid cathode
Iron disulfide (FeS_2)	Sulfur dioxide (SO_2)	Iodine (I_2)
Carbon fluoride (CF_x)	Thionyl chloride ($SOCl_2$)	Lead iodide (PbI_2)
Manganese dioxide (MnO_2) Silver chromate (Ag_2CrO_4)	Sulfur chloride (SO_2Cl_2)	Me_4NI_5-C cell Bromine trifluoride (BrF_3)
Copper oxide (CuO)		

Li-ion cells have been marketed later (Table 2.3) by several battery companies in the world (Sanyo, Matsushita, Hitachi, Yuasa, Moli, A&T, SAFT, etc.). Lithium-ion chemistries represent a significant step forward in battery technology. As an example, designed for sophisticated portable applications, the VL18650 from SAFT delivers a rated capacity of 1.2 Ah within stable operating conditions of discharge temperature in the range between −20 and +60 °C. Now, scientists and engineers have to throw down the challenge of developing high power LiBs for electric vehicles. Different varieties of Li-ion batteries were launched to power EV cars: in 1995, the 100-Ah $LiCoO_2$//graphite battery from Sony Corp. supplied energy for traveling 200 km at maximum speed up to 120 km h^{-1}; in 1996, the car launched by Mitsubishi Motors used $LiMn_2O_4$ spinel as cathode powering a trip of 250 km.

2.3 Primary Lithium Batteries

Developed in the early 1970s, primary lithium batteries are the most energy-dense electrochemical cells made for watches, film cameras, medical devices, and military purposes. Lithium primary cells have a typical gravimetric density 250 Wh kg^{-1}, against only 150 Wh kg^{-1} for Li-ion batteries. Various technologies that differ in chemistry and construction have been used to develop primary lithium batteries. In Table 2.4, they are classified into three groups, according to the form and the type of cathode and electrolyte used. Frost and Sullivan said that in 2009,

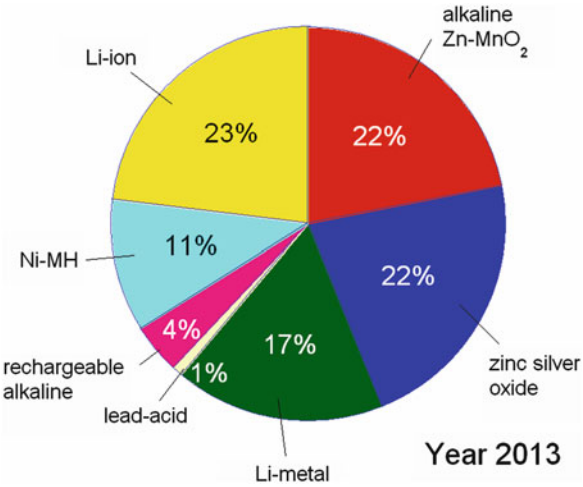

Fig. 2.1 Battery production in Japan for the year 2013. Primary batteries amounted to 61 %, including 17 % of lithium batteries

primary batteries including alkaline that were leading the market, carbon-zinc and lithium cells made 23.6 % of the global market with 3 % for primary lithium cells; it has been predicted a 7.4 % decline in 2015 due to the development of rechargeable batteries [43]. According the Freedonia's studies, the production of primary batteries doubled between 2002 and 2012. US demand for primary and secondary batteries are expected to grow 4.2 % per year to $17.1 billion in 2017. Lithium batteries will offer the best growth opportunities in both the rechargeable and primary battery segments [44]. Figure 2.1 presents the Japanese battery market in the year 2013, in which lithium-metal technology is 17 % segment of the total battery revenue.

2.3.1 High Temperature Lithium Cells

2.3.1.1 Lithium Iron Disulfide Battery

The lithium iron sulfide battery operates at about 400–500 °C using a fused halide eutectic electrolyte immobilized in the pores of a suitable separator. This battery displays a number of attractive features compared to the sodium-sulfur battery, including prismatic flat-plate construction, ability to withstand numerous freeze-thaw cycles, cell failures in short-circuit conditions, ability to withstand overcharge and low-cost materials with available construction techniques. The major disadvantage is a somewhat lower performance. This battery is suitable for load-leveling applications. Attention has also focused on battery designs suitable for electric propulsion [46]. Energizer successfully produced the first commercially available AA-size 1.5 V Li-FeS_2 battery in 1989 (specific energy density ~297 Wh kg^{-1}). The 1.5 V AAA-size followed in 2005.

The most commonly used electrolytes are the LiCl-KCl binary eutectic and the ternary LiF-LiCl-LiI lithium halides. With Li-Al alloy anode and FeS_2 cathode the discharge occurs in several discrete steps:

$$4Li + 3FeS_2 \rightarrow Li_4Fe_2S_5 + FeS, \tag{2.2}$$

$$2Li + Li_4Fe_2S_5 + FeS \rightarrow 3Li_2FeS_2, \tag{2.3}$$

$$6Li + 3Li_2FeS_2 \rightarrow 6Li_2S + 3Fe, \tag{2.4}$$

giving voltage plateaus at 2.1, 1.9, and 1.6 V, respectively. The use of Li-Al results in almost 50 % decrease in the theoretical specific energy, but much better stability is achieved. Most of the development was focussed on the LiAl/FeS couple; the Varta Battery Company (Germany) has produced a series of 140-Ah cells with a specific energy of 100 Wh kg^{-1} at a low discharge rate of 80 mA cm^{-2}, falling to 50 Wh kg^{-1} at high current density 250 mA cm^{-2}. Another version of LiAl/LiCl-LiBr-KBr/FeS_2 utilizes a dense FeS_2 electrode that only discharges to a stoichiometry corresponding to FeS (rather than to elemental Fe, which was the case of prior versions) [47]. The melting point of LiCl-LiBr-KBr at 310 °C allows cell operation at about 400 °C. These innovations have resulted in greatly improved capacity retention, and cells cycling for more than 1000 times. These cells are also developed in the USA and manufactured by Eagle-Picher, by Gould, and by SAFT America. Cells of 150- to 350-Ah capacity yield specific energies of 70–95 Wh kg^{-1} available at a 4-h discharge rate. There are still a number of unresolved scientific questions about the chemistry of LiAl/FeS cells and the mechanism of degradation and failure. In this system the separator is clearly a crucial component, which must not only keep the electrode materials apart but also allow good permeation of the electrolyte. The most suitable materials are found to be boron nitride and zirconia in the form of woven cloths, but they are obviously very expensive options.

2.3.1.2 Lithium Chloride Battery

Similar designs have been used in lithium chloride batteries, which operate at a temperature of 650 °C. The cell has the form Li(liq)/LiCl(liq)/Cl_2(g), carbon. The two electrodes, liquid Li anode and the porous carbon cathode in which the chlorine gas is fed under pressure, are separated by a molten lithium chloride electrolyte. The overall cell reaction is:

$$Li(liq) + ½\ Cl_2(g) \rightarrow LiCl(liq), \tag{2.5}$$

with an OCV of 3.46 V. This system delivers a theoretical energy density 2.18 kWh kg^{-1} at the working temperature. The most serious problems with this battery, however, are the corrosion of cell components and the development of satisfactory seals.

2.3.2 Solid-State Electrolyte Lithium Batteries

Solid-electrolyte batteries generally exhibit high thermal stability, low rates of self-discharge (shelf life of 5–10 years or better), ability to operate over a wide range of environmental conditions (temperature, pressure, and acceleration), and high energy densities of 0.3–0.7 Wh cm^{-3}. However, limitations include relatively low power density due to the high impedance of most lithium-conducting solid electrolytes. The three commercial solid electrolyte battery systems are based on the solid electrolyte LiI, either formed in situ during cell manufacture or dispersed with alumina.

2.3.2.1 Lithium-Iodine Cells

From the first pacemaker implant in 1958 by Dr Ake Senning surgeon at the Karolinska Hospital in Stockholm, numerous engineering developments have faced challenges in battery power. In 1972, a primary lithium-iodine battery replacing the mercury-zinc cells greatly extended the cardiac pacemaker life (about 10 years). More details on the history of this battery can be found in ref. [48]. The most important factor for a cardiac pacemaker battery is its reliability [49]. The terminal voltage decay characteristic is well behaved, falling slowly enough for battery end-of-life (EOL) to be anticipated in routine follow up. The lithium-iodine battery has a solid anode of lithium and a polyphase cathode of poly-vinyl-pyridine (PVP), which is largely iodine (at 90 % by weight). The solid electrolyte is constituted by a thin film of LiI. The discharge reaction is given by:

$$2\mathrm{Li} + n\mathrm{I}_2(\mathrm{PVP}) \rightarrow (n-1)\mathrm{I}_2(\mathrm{PVP}) + 2\mathrm{LiI}. \tag{2.6}$$

The cathode material is thus formed by the thermal reaction of iodine and polyvinyl-pyridine. This cell has an open-circuit voltage of 2.8 V. The theoretical specific energy for the $Li/LiI/I_2(PVP)$ cell is 1.9 Wh $cm^{-3.}$ The electrolyte ionic conductivity is $\sim 6.5 \times 10^{-7}$ S cm^{-1} at 25 °C, and the energy density is 100–200 Wh kg^{-1} [50]. The ratio of iodine to PVP is typically between 30/1 and 50/1, depending on the manufacturer. Phillips and Untereker have studied the phase diagram of the iodine/PVP material [51]. They demonstrated that at the application temperature (37 °C), the material passes through three phases—a two-phase region comprising a eutectic melt and pure iodine, a single phase liquid region, and a two-phase system wherein the iodine/monomer unit adduct phase coexists with the melt. An interesting and useful feature of the cathode material is that it is an electronic conductor. The conductivity is a function of the ratio of iodine to PVP. The maximum conductivity occurs at the I2/PVP weight ratio of 8/1. Since the initial ratio is much greater than this, the electronic conductivity increases until it reaches the weight ratio of 8/1, and then decreases gradually as the cell reaction continues. The increase in cell impedance caused by this decrease, together with the

increase due to the formation of the lithium/iodine reaction product, leads to a gradual and predictable decrease in cell voltage that is easily detected by the electronic circuitry of the pacemaker. This feature allows the clinical personnel to detect the onset of the end-of-service point of the battery well before that point is reached, making it possible to schedule replacement surgery in a timely manner by routine checking of the battery status by telemetry. The volume change accompanying the cell discharge is ~12 % if the cathode is 91 % iodide by weight. This volume change may be accommodated by the formation of a porous discharge product or by the formation of macroscopic voids in the cell. Such batteries are used as power sources for implantable cardiac pacemakers, operating at 37 °C. They are commercialized by Catalyst Research Co., Wilson Greatbatch Inc., and Medtronic Inc. The lithium-iodine batteries have extended system lives up to 10 years for 120- to 250-mAh capacities. For use as power sources for portable monitoring or recording instruments, they have a nominal capacity of 15 Ah or less, and most have deliverable capacities under 5 Ah.

Batteries of medium capacities, i.e., up to around 1 Ah, can be used for random-access memory power supplies in electronics. Similar batteries using Li//Br have also been built. The greater electronegativity of bromine gives rise to voltages the order of 3.5 V and energy densities as high as 1.25 Wh cm^{-3}. Their practical application is, however, limited by the low conductivity of the LiBr films that are formed.

2.3.2.2 Li/LiI-Al_2O_3/PbI_2 Cells

These batteries are recommended for low-rate operations and they are particularly suited for applications requiring long life under low drain or open-circuit conditions. Different cathodes have been used in these commercial solid-state cells, including a mixture of $PbI_2 + Pb$ or $PbI_2 + PbS + Pb$, and a new system under development uses a mixture of $TiS_2 + S$ or As_2S_3, which increases the energy density. The solid electrolyte is a dispersion of LiI and LiOH with alumina. Lithium ionic conductivities as high as 10^{-4} S cm^{-1} have been reported in such a dispersion at temperature of 25 °C [52]. The discharge properties are characterized by an open-circuit voltage of 1.9 V and an energy density of 75–150 Wh kg^{-1}. A three-cell battery design manufactured by Duracell International delivers 6 V and offers a capacity of 140 mAh as a pacemaker power source. In typical complementary metal oxide semiconductor (CMOS) memory applications, the 350-mAh battery can be used with 1.0-V cutoff potential.

2.3.2.3 Carbon Tetramethyl-Ammonium Penta-Iodide Batteries

The Li/LiI (SiO_2, H_2O)/Me_4NI_5 + C cells were evaluated for use in cardiac pulse generators. They exhibited a voltage of 2.75 V and were projected to have a volumetric energy density of 0.4 Wh cm^{-3} [53]. The cathode is a mixture of carbon and tetramethyl-ammonium penta-iodide (Me_4NI_5).

2.3.2.4 Lithium Bromine Trifluoride Battery

Great advances have been made on the unconventional approach of combining alkali metals with strongly oxidizing liquid, e.g., SO_2, $SOCl_2$, or BrF_3, which acts simultaneously as electrolyte solvent and cathode depolarizer. BrF_3 is a very reactive liquid at room temperature, and the concept of a Li//BrF_3 cell has appeared [45, 53, 54]. A super high energy density battery which includes a lithium anode, a catalyst with liquid bromine trifluoride, and an electrolyte of antimony pentafluoride has been invented [55]. The cell reaction proceeds by the bromine trifluoride that disproportionates according the following equation:

$$4Li + BrF_3 \rightarrow 3Li^+F^- + Li^+Br^-. \tag{2.7}$$

Consequently, no electrolyte salt is necessary because lithium was found to be stable in BrF_3 due to the formation of the protective surface layer. Upon cell activation a potential of 5 V is established, giving theoretical energy densities of 2680 Wh kg^{-1} and 4480 Wh dm^{-3}. A typical discharge of a Li/BrF_3/C cell is achieved at 5 mA cm^{-2} current density, and a capacity of 5 mAh cm^{-2} has been measured. The cell performance is controlled by the formation of the reaction product layer at the anode–electrolyte interface, leading to an increase in impedance. The BrF_3 electrolyte can also be modified by dissolution of various fluorides, e.g., $LiAsF_6$, $LiPF_6$, $LiSbF_6$, or $LiBF_4$. Such a cell is actually strongly developed by EIC Laboratories Inc. in the USA.

2.3.3 Liquid Cathode Lithium Batteries

2.3.3.1 Lithium Thionyl-Chloride Batteries

The lithium thionyl-chloride battery uses liquid thionyl chloride ($SOCl_2$) as its positive active material, and lithium metal as its negative active material [56]. The overall reaction of the battery is expressed as:

$$2SOCl_2 + 4Li \rightarrow 4LiCl + S + SO_2. \tag{2.8}$$

The Li//$SOCl_2$ battery achieves a high voltage of 3.6 V and provides high volumetric energy density of 970 Wh dm^{-3} with discharge current of 100 μA. It can be used over a wide temperature range from −55 to +85 °C. This cell displays remarkably lower self-discharge than conventional batteries owing to the formation of a LiCl protective layer over the Li-metal anode surface. Main applications of Li//$SOCl_2$ batteries are: medical instruments, cash registers, measuring instruments, onboard microcomputers, sensors, electronic meters (gas, water, electricity, etc. Bipower® commercialized Li//$SOCl_2$ batteries with nominal voltage 3.6 V. The 1.6-Ah prismatic cell (BL–16PN-64) can be discharged at continuous current

20 mA. Applications include RF transmitters, military GPS systems, data loggers, alarm and security systems, CMOS memory backup and medical equipment. Li//$SOCl_2$ batteries from SAFT are bobbin (LS) or spiral (LSH) cells that operate at 3.6 V and show lowest self-discharge for extended operating life in the temperature range −60 to +150 °C. LS cells are designed specifically for long-term (5–20+ years) applications featuring a few μA base currents and periodic pulses, typically in the (−150 mA range, while. LSH cells are designed for applications requiring continuous current in the range 0.1–0.8 A. Taridan Batteries GmbH commercializes the SL-500 Li//$SOCl_2$ series exhibiting an extended temperature range up to +130 °C. These batteries have excellent shelf life (10 years) and extremely low self-discharge (1 % or less per year).

2.3.3.2 Lithium-Sulfur Dioxide Batteries

The cathode of the lithium-sulfur dioxide (Li-SO_2) batteries consists of a gas under pressure with another chemical as electrolyte salt; this is analogous to the thionyl chloride electrolyte and its liquid cathode [57]. Applications of these systems include emergency power units for aircraft and military cold-weather applications (e.g., radio operation). NASA is using Li-SO_2 cells for balloon and flight equipments. Features of Li-SO_2 batteries are as follows [58]: (1) high energy density up to 280 Wh kg^{-1}, (2) open-circuit voltage 2.95 V, operation voltage is between 2.7 and 2.9 V depending upon loading resistance, (3) long storage life, less than 2 % of self-discharging rate per year, could be stored for 10 years at room temperature, (4) spiral-wound construction may be discharged at higher rates, and (5) wide operation temperature range, −54 to +71 ° C. Spiral-wound Li-SO_2 battery from SAFT operates at 3 V in the temperature range −40 to +70 °C. This battery shows excellent capacity above 1 A. Its main advantage is the superior power at −40 °C and the low-self discharge during storage. The 11.5-Ah cell (model LO39SHX) can deliver 60 A maximum pulse discharge rate.

2.3.4 Solid Cathode Lithium Batteries

The semiconductive properties and tunnel structure of sulfide and transition-metal oxides led to the use of these materials in lithium power sources (Table 2.5). Several lithium-based chemistries were successfully applied to replace the prior system Zn/AgO and later the lithium-iodine batteries in implantable medical devices [59–61]. For example, Li//CuO, Li//V_2O_5, Li//CF_x, and more recently Li//$Ag_2V_4O_{11}$ couples have been adopted to power cardiac pacemakers requiring less that 200 μW [62, 63]. The lithium/carbon monofluoride (Li//CF_x) primary cells are very attractive in several applications because of the double energy density with respect to the state-of-the-art Li//MnO_2 primary batteries (theoretically 2203 against 847 Wh kg^{-1}).

Table 2.5 Primary lithium batteries with solid cathodes

Systems	OCV (V)	Comments
Li//CF_x	3.1	Developed by Matsushita (1973)
Li//MnO_2	3.3	Sanyo (1975)
Li//Ag_2CrO_4	3.25	For implanted pacemakers
Li//CuS	2.0–1.5	Two voltage plateaus
Li//CuO	2.4	Can operate at 150 °C
Li//FeS_2	1.8	Variant is Li//$CuFeS_2$
Li//$Ag_2V_4O_{11}$	2.75–2.50	For implanted pacemakers

2.3.4.1 Lithium Polycarbon Fluoride Cells

Polycarbon fluorides of the general formula $(CF_x)_n$ can be obtained by direct fluorination of carbon black or other varieties of carbon at high temperatures. Theoretical specific energy density 2600 Wh kg^{-1} can be achieved with these materials. Lithium cells with polycarbon fluoride cathodes have an open-circuit voltage in the range of 2.8–3.3 V, depending on the composition of the cathode material. A typical cell reaction may be written [64]:

$$nx\mathrm{Li} + (\mathrm{CF}x)n \rightarrow n\mathrm{C} + nx\mathrm{LiF}. \tag{2.9}$$

Thus, the theoretical specific discharge capacity Q_{th} (in mAh g^{-1}) is expressed by:

$$Q_{\mathrm{th}}(x) = \frac{xF}{3.6(12 + 19x)}. \tag{2.10}$$

The graph in Fig. 2.2 displays the experimental specific capacity of the $(CF_x)_n$ materials as a function of the stoichiometry ($0.5 \leq x \leq 1.0$). The theoretical capacity is calculated according to Eq. (2.11).

The crystal structure of graphite fluorides $(CF_x)_n$ compounds with $x > 0.5$ was investigated by Touhara et al. who proposed two phases: a stage-1 $(CF_1)_n$ and a stage-2 $(CF_{0.5})_n$, also commonly referred to as $(C_2F)_n$ [65]. In stage-1 compounds, the fluorine is intercalated between each carbon layers to yield –CFCF- layers stacking, whereas in stage-2 (hexagonal, C_{3h} symmetry) according to their model, fluorine occupies every other layer with a stacking sequence of –CCFCCF–. The hexagonal symmetry is preserved in both $(CF_1)_n$ and $(CF_{0.5})_n$ phases. Theoretical crystal structure calculations were also carried out and different layers stacking sequences were compared from their total energy. Due to electron localization in the C–F bond, a huge drop of the electrical conductivity occurs ~10^{-14} S cm^{-1} in $(CF)_n$ compared with ~1.7×10^4 S cm^{-1} in graphite.

Cells based on polycarbon fluorides are manufactured commercially in various forms. System developed by Matsushita Electric Industrial Co. is designed as a BR 435 cylindrical cell. Cells constructed by Nippon Steel Co. use carbon fibers as electrodes; they are found to be rechargeable. Cells for military applications have

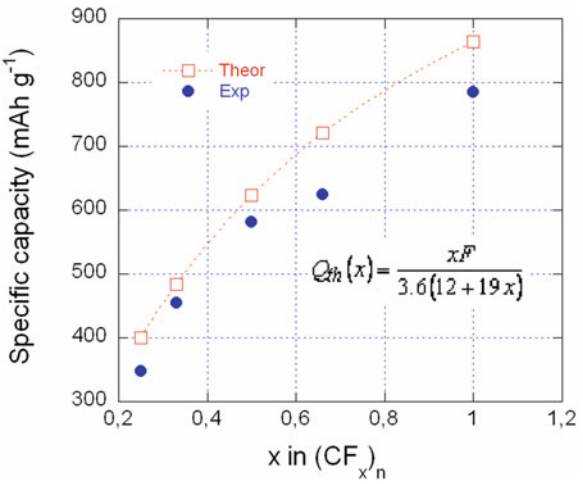

Fig. 2.2 Composition dependence of the experimental theoretical specific capacity of $(CF_x)_n$ cathode materials for primary lithium batteries. The theoretical capacity is calculated according to Eq. (2.11)

been produced in the USA by Eagle Picher and by Yardney Electric. There are spiral-wound cylindrical cells with a largest cell capacity of 5 Ah.

Lam and Yazami prepared sub-fluorinated graphite fluorides $(CF_x)_n$ compounds $(0.33 < x < 0.63)$ from natural graphite. The cathode behavior in lithium batteries investigated under low discharge rate shows that the energy density increases with the fluorine content x. However, at higher rates, sub-fluorinated compounds performed better than commercial $(CF_x)_n$ synthesized from petroleum coke. Specific capacity 400 mAh g^{-1} was obtained for Li//$CF_{0.52}$ coin cell discharged at 2.5*C* [66]. The rate capabilities of Li//$(CF_x)_n$ 18650-type 3.6-Ah cells using 1 mol L^{-1} $LiBF_4$ in EC:PC:EMC (1:1:3) as electrolyte were tested at Sandia Natinal Labs in the temperature range −40 to +72 °C [67]. The Li//CF_x system was fabricated by Wilson Greatbatch as an alternative electrical source for advanced pacemaker systems [68]. Li//CF_x-MnO_2 hybrid cells are commercialized by Ultralife. These cells are fabricated for at least 15 years shelf life and deliver 40 % or more capacity than the same-sized Li//MnO_2 system. Li//CF_x is estimated to be ~9 % of the world's primary battery market that is mainly shared by Panasonic (50 %), Greatbatch Medical (20 %), Spectrum Brands (20 %) and Eagle-Picher [69].

2.3.4.2 Lithium Manganese Oxide Batteries

Lithium manganese oxide (Li-MnO_2) battery is the most common consumer grade battery that covers about 80 % of the lithium battery market. This system includes heat-treated MnO_2 as cathode, lithium metal as anode and $LiClO_4$ in propylene carbonate/dimethoxyethane as aprotic electrolyte. The overall battery reaction is:

$$Mn^{IV}O_2 + Li \rightarrow Mn^{III}OOLi. \tag{2.11}$$

The cell reaction involves reduction of the MnO_2 without gases exhaustion and the product remains in the cathode. The system Li-MnO_2 displays several advantages: (1) the energy density is 150–250 Wh kg^{-1} and 500–650 Wh dm^{-3}, (2) the operating temperature ranges from −40 to +60 °C, (3) manganese dioxide is a low cost and safe material. Batteries are leading the market at approximately 50 % as estimated by Frost and Sullivan.

Many companies (Panasonic, Sony Energytec, Sanyo, Fuji, NTT, Matsushita, Varta, SAFT, etc.) embarked on ambitious programs to develop small rechargeable high-energy density, low cost Li-MnO_2 cells. Panasonic sales various battery sizes, from 30-mAh coin cells (CR1025) to cylindrical 2.4-Ah batteries. Duracell® Li/MnO_2 batteries are being used in a wide range of applications, from powering all functions of fully automatic 35-mm flash cameras to providing long-term standby power for computer clock/calendars. The button cell and spiral-wound cylindrical cell Maxell® Li//MnO_2 batteries have long-term reliability of 10 years; self-discharge rate is about 0.5 % per year. The cylindrical-type CR17450 model weighting 22 g has a nominal capacity 2500 mAh, $V_{oc} = 3$ V, and operates in the temperature range −40 to +85 °C. Typical voltage profiles of Li//MnO_2 batteries during discharge continuously at 40 mA are shown at different temperatures in Fig. 2.3 (from Maxell flyer). Scrap Li//MnO_2 batteries by Energizer® meet US Department of Transportation (DOT) requirements of the 49CFR173.185 standard: limit of 12 g of Li per cell, strong outer packaging, external short circuits prevented. Sony has commercialized a button-type CR2025 cell tested at 23 °C under a load of 15 kΩ for 900 h. Excellent long-term storage reliability was demonstrated: at 60 °C for 120 days is the equivalent of storage at room temperature for 6 years. PowerStream fabricate CR series of primary Li//MnO_2 button cells with nominal capacity from 25 to 1000 mAh. The price of the CR2477 1 Ah-cell is $3.00. The cylindrical Li//MnO_2 3-V battery by Bipower® (model CR34615) of nominal capacity 8 Ah weights 120 g. Panasonic sells a varieties of light button cells; the

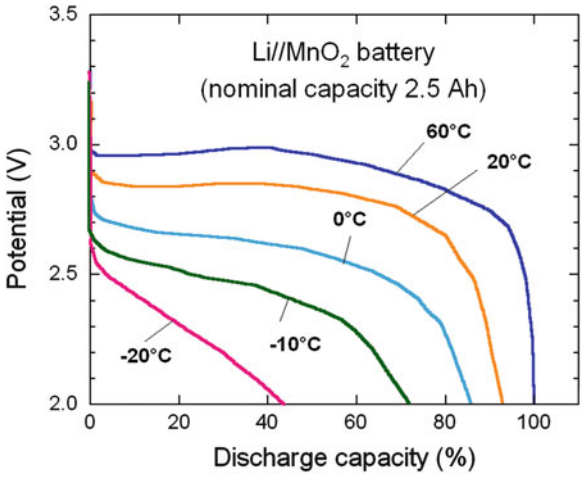

Fig. 2.3 Typical voltage profiles Li//MnO_2 batteries discharged continuously at 40 mA at different temperatures

CR2025 items of capacity 165 mAh weight 2.3 g. Since 1976, Sanyo Electric Co. has developed a wide variety of primary Li-MnO_2 cells to meet the demands of a large diversified market. Coin-type CR1220 36-mAh cell weighting 0.8 g delivers a maximum continuous discharge current 2 mA. The high-power cylindrical 2.6-Ah cell (spiral structure) weighting 23 g delivers 500 mA.

2.3.4.3 Low Temperature Lithium Iron Batteries

Room temperature primary Li//FeS_2 batteries use nonaqueous electrolyte, such as a lithium/iron disulfide, with good low temperature performance characteristics. The electrolyte has a solute including lithium iodide dissolved in an ether-containing solvent including a 1,2-dimethoxypropane based solvent component and no more than 30 vol% 1,2-dimethoxyethane [70, 71]. Commercial Li//FeS_2 AA primary batteries have offered substantially longer runtime than equivalent sized Zn//MnO_2 alkaline AA cells for high-power applications and below ambient temperature [72]. The electrolyte consisted of 1 mol L^{-1} $LiCF_3SO_3$ dissolved in 24.95 vol.% dioxolane, 74.85 vol.% dimethoxyethane, and 0.2 vol.% dimethylisoxazole. However, the rate capability of commercial Li//FeS_2 batteries may be limited by the ion conductivity of the electrolyte when FeS_2 samples have crystal sizes smaller than 1 μm. It has been demonstrated that the electrochemical performances are strongly dependent on the FeS_2 cathode particle size. Reducing crystal size of FeS_2 from 10 μm down to 100 nm increases the presence of crystal boundaries or surfaces per unit volume of FeS_2, provides a large number of nucleation sites for lithiated products, and thus promotes the kinetics of the heterogeneous (not intercalation) lithiation process of FeS_2 [73]. For a loading cathode of 14 mg cm^{-2}, the discharge voltage profiles of Li//nano-FeS_2 cells show a two-voltage-step reaction at 1.7 and 1.5 V at current densities lower than 3 mA g^{-1} (0.042 mA cm^{-2}). The 1.7-V lithiation plateau was attributed to the formation of pyrrhotite $Fe_{1-x}S$ ($0 < x < 0.2$) and $Li_{2+x}Fe_{1-x}S_2$ ($0 < x < 0.33$) intermediate phases, and the 1.5 V reaction produced a mixture of plate-shaped Li_2S and amorphous Fe as final products.

2.3.4.4 Silver Vanadium Oxide Cells

$Ag_2V_4O_{11}$ (SVO) is an interesting cathode material for lithium primary batteries used as a power source for implantable cardiac defibrillators (ICDs). Li//SVO cells have traditionally been designed by Medtronic Inc. to discharge the cathode to a composition of $>6Li:Ag_2V_4O_{11}$ [74]. The SVO tunnel-like structure (C-centered monoclinic) consists of vanadium oxide layers with silver located between the layers. Li//SVO batteries have a distinctive discharge curve with two plateaus, one at 3.24 V and one at 2.6 V. In the fully discharged state, the composition of the cathode is $Li_6Ag_2V_4O_{11}$. This composition corresponds to reduction of silver to Ag^0 and reduction of V^{5+} to V^{4+} [75, 76]. Lithium batteries with hybrid cathodes of $Ag_2V_4O_{11}$ and CF_x have been developed by Medtronic Inc. that combine the best

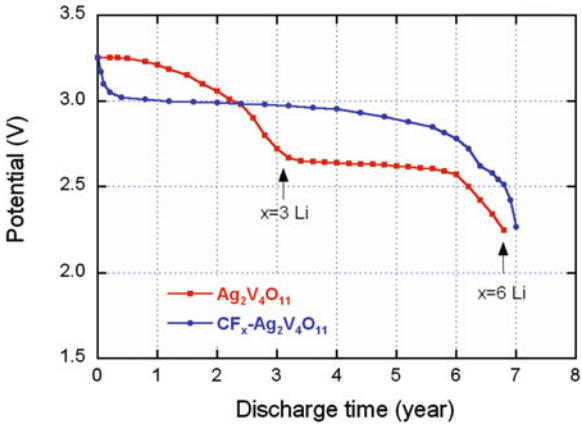

Fig. 2.4 The discharge profile of Li//SVO and Li//SVO-CF_x composite cells used to power medical devices

features of both cathode components. Figure 2.4 compares the discharge profile of Li//SVO and Li//SVO-CF_x composite cells. Silver chromate, Ag_2CrO_4 was also used as a cathode material in Li primary battery for pacemaker. The cell reaction is identical to that of SVO with the formation of metallic silver and final solid product Li_2CrO_4. The nominal voltage is 3.5 V and the specific energy is 200 or 575 Wh dm^{-3} for a 2.5-V cutoff. Button cells were produced by SAFT.

2.3.4.5 Other Primary Lithium Batteries

In many cases the discharge mechanisms involved in lithium oxide cells are still not fully understood. The discharge reaction can be described as a formal displacement process:

$$2\mathrm{Li} + MO \rightarrow \mathrm{Li_2O} + M, \tag{2.12}$$

where MO is an oxide such as CuO, Mn_2O_3, Bi_2O_3, or Pb_3O_4 with theoretical capacity of 670, 310, 350, and 310 mAh g^{-1}, respectively. OCV are in the range 3.0–3.5 V and a practical energy density of 500 Wh dm^{-3} is obtained. Varta has developed a CR 2025-type cell and SAFT has manufactured an LM 2020-type cell. The Li//CuO button cell (LC01) constructed by SAFT exhibits a single step which may be attributed to the simple displacement reaction (Eq. 2.12). This Li//CuO cell delivers an OCV of 1.5 V and has the highest specific energy of all solid cathode-based lithium cells. Practical value of 750 Wh dm^{-3} is obtained. The liquid electrolyte varies from manufacturer to manufacturer, but $LiClO_4$ in dioxolane is very often used. The cylindrical cells manufactured by SAFT have practical capacities in the range 0.5–3.9 Ah.

Sulfide electrodes have the advantage over the corresponding oxides that most of them are good electronic conductors, so that sulfide-based batteries usually do not

require the addition of carbon into the cathode. Batteries based on cupric sulfide cells (three in series) have been developed for use in a cardiac pacemaker. Li//CuS undergoes in two steps, so that the discharge curve exhibits two plateaus at 2.12 and 1.75 V during the first discharge to 1.5 V with a capacity of 530 mAh g^{-1}. The reduction of CuS results in the formation of Li_xCuS during the first voltage plateau, and $Cu_{1.96}S$, Li_2S and metallic Cu during the second voltage plateau [77].

2.4 Secondary Lithium Batteries

Basically, the idea of using materials that undergo insertion reactions as the electrochemically active component at the positive electrodes began to be explored in the 1970s, giving birth to the rechargeable lithium batteries (RLB). Two approaches consist in the design of RLB as shown in Fig. 2.4. The first system utilizes an insertion compound as positive material and a lithium-metal foil as the negative electrode, the so-called lithium-metal battery (Fig. 2.4a). The second system consists in using two open-structured materials as electrodes, in which the lithium ions can be shuttled from one intercalation compound acting as lithium-ion source to another receiving lithium-ion and vice versa for the discharge process. This is the commonly known lithium-ion battery (Fig. 2.4b) that was initially named "rocking chair battery," "swing battery" or "shuttlecock battery." Sometimes, LiBs are also named "lithium metal-free rechargeable batteries" [10] (Fig. 2.5).

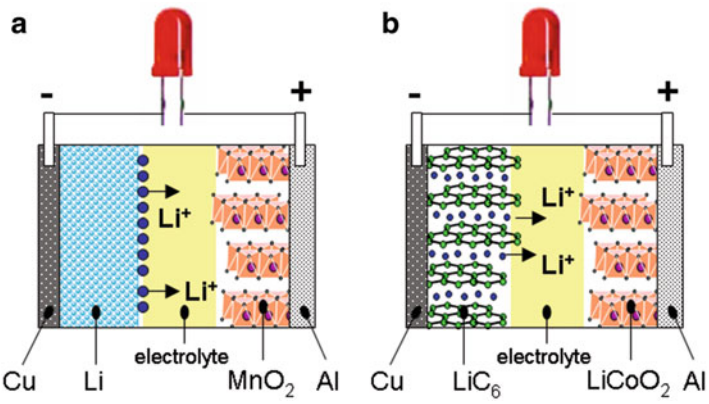

Fig. 2.5 Schematic representation of rechargeable lithium batteries. There are two systems according the nature of the negative electrode either Li metal (**a**) or Li insertion compound (**b**). In both cases, the positive electrode is constituted by an insertion compound, in which the redox reaction occurs at high potential versus Li^0/Li^+

2.4.1 Lithium-Metal Batteries

The first electrochemical applications of intercalation compounds appeared on lithium-metal batteries (LMBs). The idea of using materials that undergo insertion reactions as the electrochemically active components of batteries began to be explored and accepted in the early 1970s [8]. Of particular interest was the case of an electron donor mechanism that takes place in transition-metal dichalcogenides MX_2 ($X = S$, Se). The prototype is the Li//Li_xTiS_2 system [24]. Then, a series of studies of the transition metals of the first and second row were reported. Basically, batteries using MX_2 compounds can be considered as concentration cells, in which the activity of lithium varies in the composition range $0 \leq x \leq 1$. For $x = 0$, TiS_2 is at the pristine state and the cell is fully charged, while, for $x = 1$, the fully intercalated $LiTiS_2$ state corresponds to the discharged state. In Li_xTiS_2, for instance, the inherent reversibility of intercalation mechanism suggests the following reactions

$$xLi^+ + xe^- + TiS_2 \leftrightarrows Li_xTiS_2. \tag{2.13}$$

As the intercalation of lithium occurs as ionic species Li^+, the electro-neutrality of the host is maintained by the ejection into the external circuit of an electron generated by a reduction reaction of the transition-metal cation, the oxidation state of which switches from Ti^{4+} to Ti^{3+}. The cell potential decreases upon the Li uptake into the host framework, which follows the simple Nernst equation:

$$V(x) = E^0 - \frac{RT}{F} \ln a(Li^+), \tag{2.14}$$

where $a(Li^+)$ is the activity of Li^+ ions in Li_xTiS_2. Note that the decrease of the cell potential with increasing of Li^+ ion activity is a typical feature of Li-intercalation batteries. In the limits of the structural stability of the host, the electrochemical reaction is fully reversible.

Whittingham reported that the reversibility of the Li//TiS_2 couple permitted deep cycling for close to 1000 cycles with minimal capacity loss, less than 0.05 % per cycle, with excess lithium anode [78]. Two noticeable batteries with LiAl anode [79] that improves the safety were constructed by Exxon: the LiAl//TiS_2 cells were commercialized to power small devices such as watches and the largest lithium-metal prismatic-type cell using a $LiB(CH_3)_4$ salt in dioxolane was exhibited at the Electric Vehicle Show in Chicago en 1977 [78]. Because TiS_2 is a degenerate semiconductor that exhibits a high electronic conductivity, the use of this compound as cathode does not require the fabrication of composite electrode including conductive additive like carbon black. Despite the excellent performance of TiS_2, the great efforts of the Exxon'group were in vain, due to the formation of dendrites at the metallic anode in liquid electrolytes upon the cycling process, which is related to the non uniform change in the morphology of the anode surface as shown in Fig. 2.7. As pointed out by Xu [80], serious safety hazards are often

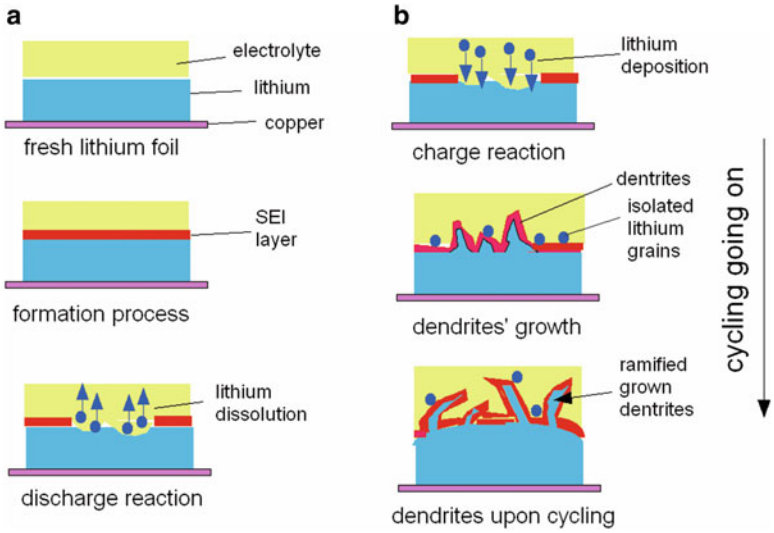

Fig. 2.6 Sketch of the formation of dendrites and deposition of lithium grains at the surface of the electrode (**a**) for the first discharge process with formation of the SEI and (**b**) upon cycling

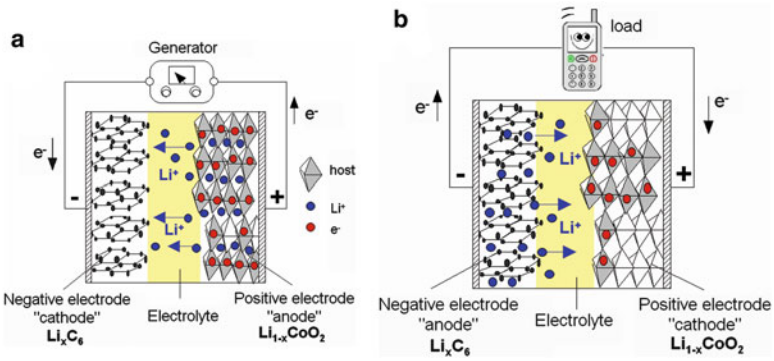

Fig. 2.7 Principle of the lithium-ion battery (**a**) charge process, (**b**) discharge process

caused by the generation of both dendrites and isolated lithium crystals (Fig. 2.6). The former creates internal shorts, and the latter is chemically active with the electrolyte solvents due to the huge surface areas of these lithium crystals. For the first discharge, that is the formation process, a passivation layer is formed at the surface of the lithium anode; this the solid electrolyte interphase (SEI), which is a poor ionic conductor in nature (Fig. 2.6a). This SEI is also growing upon repeated cycles. After the departure from the anode surface during discharge, the Li particles migrate to the cathode; the phenomenon is reverse for the charge. The deposition of Li^+ ions coming from the cathode participates to the nucleation of dendrites,

because particles do not have memory to seat back on the same site as before (Fig. 2.6b). Finally, the continuous dissolution and dendrite formation occur at the expense of the mechanical stability of the anode, which damages the whole battery operation.

The use of LMBs remains inefficient because several factors that are: (1) the unresolved control of the reactivity of lithium toward electrolyte, (2) the difficult mastery of the SEI layer, (3) the formation of large dendrites causes internal short circuiting, and (4) the increasing surface area upon cycling poses risks of overheating. It is a fact that LMBs have low coulombic efficiency ~90 % with carbonate solvents, and low cycle life due to the ceaseless growth of the passivation layer [81]. Von Sacken et al. [82] reported the thermal runaway of anode materials and showed that reactions between lithium metal and electrolyte are exothermic. These aspects are developed in the following, in the chapter related to anode materials.

Beside TiS_2, several transition-metal chalcogenide MX_2 or MX_3 ($X = S$, Se) compounds with a layered structure (case of MX_2) of one-dimensional structure ($NbSe_3$ has been the model system for quasi-1D charge density waves) have been studied as cathode materials in LMBs. Most of them display a single-phase behavior upon lithium intercalation. Li_xVSe_2 is the unique material showing a two-phase behavior that is evidenced by the appearance of two voltage plateaus in the discharge curve [83]. Three systems had emerged using TiS_2, MoS_2 and $NbSe_3$. A solid state battery Li/chalcogenide glass/TiS_2-carbon was developed at Eveready Battery Co. (USA) with the target of CMOS memory backup market. The electrolyte is a phosphorous chalcogenide glass $Li_8P4_{0.25}S_{13.75}$ mixed with LiI and on a composite electrode of TiS_2-solid electrolyte-black carbon with percentages in weight 51:42:7. The capacity ranges from 1.0 to 9.5 mAh. The cell packaging is a standard-sized XR2016 coin cell. The resistance of the cell at 21 °C is between 25 and 100 Ω depending on the state of charge [84]. A spirally wound AA-size Li/TiS_2 cell was constructed by Grace Co. (USA). At 200-mA discharge rate, a capacity of l Ah is delivered to 1.7 V [33]. Capacity of 1.6 Ah is obtained from a *C*-size Li/TiS_2 cell built by EIC Laboratories Inc. (USA). This cell operates in the temperature range from −20 to +20 °C [34]. *C*-size 3.7-Ah Li/MoS_2 batteries were especially manufactured by Moli Energy Ltd. (Canada) as the power source for pocket telephones in Japan. This battery uses a lithium anode, a propylene carbonate-based electrolyte solution and a processed MoS_2 cathode. Sustained drain rates of several amperes at a cell voltage between 2.3 and 1.3 V are obtained. The energy density is in the 60- to 65-Wh kg^{-1} range at a discharge rate of *C*/3 (approximately 800 mA) [85]. The Li-$NbSe_3$ system, termed FARADAY cell [86] was developed at AT&T (USA). The AA-size cylindrical cell was designed for operating over 200 cycles at a typical current of 400 mA to a cutoff capacity of 0.7 Ah. The ability to incorporate 3Li per $NbSe_3$ gives a relatively high theoretical energy density of 1600 Wh dm^{-3}. A practical energy density of 200 Wh dm^{-3} was achieved with the possibility of 350 cycles of charge–discharge.

It has long been recognized that lithium can be inserted chemically into metal oxide frameworks. Both molybdenum oxides [87, 88] and vanadium oxides [89] were synthesized for this purpose. The reversibility of insertion reaction in these alkali

metal bronzes Li_xMO_y formed in electrochemical cells allows many of these cells to be rechargeable. Labat et al. [90] disclosed a rechargeable cell having a cathode based on V_2O_5. A C-type Li//V_2O_5 1.4-Ah cell has been commercialized by SAFT. This cell includes a lithium or lithium alloy anode so that the cell is charged to 3.8 V. In the cell constructed by Tracor Applied Science Inc. about 2–20 % by weight of carbon is admixed to V_2O_5 [91]. The Li//V_2O_5 coin cell developed by Matsushita Micro Battery Corp. (Japan) provides power to electronic equipments like memory backup. The cathode is a mixture of V_2O_5 and 5 wt% carbon black. During the discharge, a depth of 3Li per V_2O_5 is obtained with an average voltage about 2 V. This battery delivers a capacity of 36 mA at a discharge rate of 1 mA [92].

2.4.2 Lithium-Ion Batteries

2.4.2.1 Principle

Basically, a lithium-ion battery (LiB) does not contain lithium metal, but only charge species Li^+ ions. These ions swing from one electrode to another throughout the electrolyte that is a good ionic conductor and an electronic insulator. Let us consider the charge and discharge reaction for a LiB with the Li_xCoO_2/$LiPF_6$-EC-DMC/Li_xC_6 electrochemical chain as shown in Fig. 2.7. A fresh cell is in the discharge state, i.e., at low potential. Consequently, in the initial state, the positive electrode framework is full of Li^+ ions (Li_1CoO_2), while the anode is empty (carbon C). As any electrochemical reaction implies the transport of ions and electrons, the redox process in a LiB is as follows. During the charge process, Li^+ ions are generated by the positive electrode (anode at this time), migrate across the electrolyte and penetrate the negative electrode (cathode at this time), while electrons circulate through the external circuit; in the process, the positive electrode is oxidized losing x electrons ($Li_{1-x}CoO_2$) and the negative electrode is reduced capturing x electrons (Li_xC_6) and vice versa for the discharge process.

For a LIB made of $LiCoO_2$ as positive electrode and graphite-like carbon as negative electrode, the chemical reactions for charge and discharge are expressed as shown below:

$$x\mathrm{Li}^+ + xe^- + 6\mathrm{C} \leftrightarrows \mathrm{Li}_x\mathrm{C}_6(\text{at the negative}), \tag{2.15}$$

$$\mathrm{LiCoO}_2 \leftrightarrows \mathrm{Li}_{1-x}\mathrm{CoO}_2 + x\mathrm{Li}^+ + xe^-(\text{at the positive}), \tag{2.16}$$

where the upper arrow represents the discharge process and the lower one the charge process. The overall battery reaction is expressed as:

$$\mathrm{LiCoO}_2 + 6\mathrm{C} \leftrightarrows \mathrm{Li}_{1-x}\mathrm{CoO}_2 + \mathrm{Li}_x\mathrm{C}_6. \tag{2.17}$$

Note that the $LiCoO_2$//C-type cell operates at high voltages, around 4 V, due to the big difference $[\mu(\mathrm{LiCoO_2}) - \mu(\mathrm{C})]$ between the chemical potentials of the electrodes (Eq. 1.2).

Table 2.6 Characteristics of Li-ion against NiMH cell

Characteristics	Ni-MH	Li-ion
Operating voltage (V)	1.3	3.7
Specific energy (Wh kg^{-1})	75	160
Self discharge (% per month)	30	5
Cycle life	Good	Good
Memory effect	Yes	No

Currently, the electrolyte is a mixture of alkyl carbonate solvents (aprotic) with lithium hexafluophosphate salt ($LiPF_6$) to provide ionic conductivity for the back and forth motion of the lithium ions. Generally the transport of ions into a solid-state compound is a slow process that requires optimization by using very well crystallized electrode materials [93, 94]. However, some amorphous substances can be used and this area is receiving increasing attention, in particular in the case of some anode materials that are discussed in Chap. 10. An important strategy in the design and optimization of an electrode is the use of the nanotechnology to reduce the size of active particles as small as possible. The smaller the particle size, the shorter the length of the path of a guest species in the solid, and the smaller the change from the core to the surface of individual particles during discharge–charge cycling [95].

Lithium ion batteries have a high energy density and are ideal for cyclic applications. They allow savings in volume and weight up to 70 % compared to traditional lead acid batteries or Ni-MH batteries (see Table 2.6). One disadvantage of the Li-ion batteries is that Battery Management System (BMS) is inevitable, to control and monitor the battery pack, and automatically compensate imbalances between cells as much as possible. This ensures a constant high capacity and a long life span. The BMS must also test constantly each cell to avoid thermal runaway and the propagation to other cells (battery fires). However, the recent investigations of LiBs with iron phosphate and titanate electrodes have shown the LFP/LTO cell passes successfully the battery tests for safety use in public transportation [96], in which case the role of the BMS is reduced to the control of the balance between the cells in the battery pack. The "18650" battery prepared under such conditions delivers a capacity of 800 mAh. It retains full capacity after 20000 cycles performed at charge rate 10*C* (6 min), discharge rate 5*C* (12 min), and retains 95 % capacity after 30000 cycles at charge rate 15*C* (4 min) and discharge rate 5*C*, both at 100 % depth of discharge (DOD) and 100 % state of charge (SOC). Since the introduction of LiBs using $LiCoO_2$ as the oxidant electrode, several new cell chemistries have been developed and used in commercial batteries.

2.4.2.2 Energy Diagram

The open-circuit energy diagram of a lithium battery has been discussed by Goodenough and Kim [97]. Figure 2.8 represents the energetic configuration of electrodes and electrolyte of a lithium battery at the thermodynamic equilibrium. The anode and cathode electrodes are electronic conductors with electrochemical

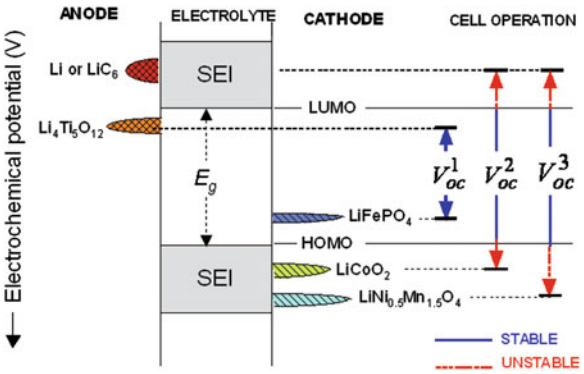

Fig. 2.8 Electronic band diagram of Li-ion batteries with various electrodes: olivine $LiFePO_4$, lamellar $LiCoO_2$, and spinel $LiNi_{1/2}Mn_{3/2}O_4$ as cathodes and lithium-metal and carbon as anodes. E_A and E_C represent the Fermi level of anode and cathode respectively. E_g is the electrolytic window that ensures the thermodynamic stability, while $E_A > E_L$ and $E_C < E_H$ requires a kinetic stability by the formation of an SEI layer

potentials μ_A and μ_C, also called Fermi level energies E_A and E_C, respectively. The electrolyte is an ionic conductor with a band gap E_g, which represents the separation between the lowest unoccupied molecular orbital (LUMO) of energy E_L and the highest occupied molecular orbital (HOMO) of energy E_H. The thermodynamic stability of a lithium cell requires that the electrochemical potentials of electrodes E_A and E_C are located within the energetic window of the electrolyte, which constrains the cell voltage V_{oc} of the electrochemical cell to

$$eV_{oc} = E_C - E_A \geq E_g, \tag{2.18}$$

where e is the elementary electronic charge and $E_g = E_L - E_H$ [14].

It has been suggested that in practical nonaqueous lithium battery systems the anode (Li or graphite) is always covered by a surface layer named the solid electrolyte interphase (SEI), 1–3 nm thick, which is instantly formed by the reaction of the metal with the electrolyte (this is called "formation cycle"). This film, which acts as an interphase between the metal and the solution, has the properties of a solid electrolyte. The SEI acts as a passivating layer at the electrode/electrolyte boundary gives a kinetic stability to the cell only when the condition in Eq. (2.18) is fulfilled. Otherwise, this layer has a corrosive effect and grows with the cycling life of the battery [98]. The design of electrodes must match the LUMO and HOMO level of the electrolyte. In Fig. 2.8, we present the schematic energy diagram of Li-ion cells for three different chemistries that illustrate the different situations: titanate spinel-iron phosphate (LTO//LFP), graphite-lithium cobaltate (C//LCO) and graphite-nickel-manganese spinel (C//LNM). For the couple $Li_4Ti_5O_{12}$// $LiFePO_4$, the voltage cell V_{oc} is smaller than E_g. Therefore, no SEI is formed because the electrode energy levels E_C and E_A match well within the electrolytic window, which insures very high safety. However, the price to be paid is a lower

Table 2.7 The most popular Li-ion technologies developed so far

Acronym	Cathode	Anode	Cell voltage (V)	Energy density (Wh kg^{-1})
LCO	$LiCoO_2$	Graphite	3.7–3.9	140
LNO	$LiNiO_2$	Graphite	3.6	150
NCA	$LiNi_{0.8}Co_{0.15}Al_{0.05}O_2$	Graphite	3.65	130
NMC	$LiNi_xMn_yCo_{1-x-y}O_2$	Graphite	3.8–4.0	170
LMO	$LiMn_2O_4$	Graphite	4.0	120
LNM	$LiNi_{1/2}Mn_{3/2}O_4$	Graphite	4.8	140
LFP	$LiFePO_4$	$Li_4Ti_5O_{12}$	2.3–2.5	100

open-circuit voltage, i.e., 2 V against 4 V for the graphite//$LiCoO_2$ battery. For the graphite//$LiCoO_2$ cell, graphite has E_A lying above the LUMO of used nonaqueous electrolytes and E_C of the cathode lies below the HOMO level. Consequently, the use of both graphite and $LiCoO_2$ electrodes is possible because this combination allows for the growth of the passivating SEI film. The SEI requires properties as follows: (1) it must have good mechanical stability when changes in electrode volume occur upon cycling life, (2) it must allow for fast Li^+-ion transfer from the electrolyte to the electrode, and (3) it must have a good ionic conductivity over the temperature range $-40 < T < 60$ °C [99]. In the case of the graphite//$LiNi_{1/2}Mn_{3/2}O_4$ cell, the situation is worse because E_C lies far from E_H that makes the electrode-electrolyte very instable. Table 2.7 lists a selection of the most popular Li-ion technologies that have been developed so far.

The characteristics of the cathode and anode elements together with a discussion on their advantages and disadvantages are reported in following chapters of this book. In Table 2.7, however, only the $Li_4Ti_5O_{12}$ (LTO) material is reported as an alternative to graphite, since it is being commercialized. LTO has been considered as a viable 1.5 V anode material since some time due to several advantages (see Chap. 10), and LiBs with this anode and various cathodes have been tested, starting with the LTO//$LiMn_2O_4$ combination, with liquid [100] or solid polymer [101] electrolytes. Then, the combinations LTO//$LiNi_{0.8}Co_{0.2}O_2$ and LTO//$LiCoO_2$ have been explored [102], demonstrating their viability for high-power applications. However, the exploration of LTO-based batteries was more or less abandoned for some years, due to the focus of all the research on only one parameter: the energy density and LTO suffered from the lower operating voltage. The interest in LTO was revived by the Ohzuku group [103, 104] who showed that a combination of LTO with a Li mixed oxide as cathode can deliver gravimetric energy densities as high as 250 Wh kg^{-1} and volumetric energy densities of 970 Wh dm^{-3}. The LTO//$LiMn_2O_4$ cell delivers a reversible capacity 90–100 mAh g^{-1} when cycled at 55 °C at 1*C* rate [105, 106]. With LTO particles of diameter 20 nm, the nano-LTO//$LiMn_2O_4$ cell can be cycled up to 1000 cycles at 25 and 55 °C and fast-charge capability was reported [107] up to 80*C* rate. The best results for the LTO//$LiMn_2O_4$ cell have been obtained with micrometer sized (~0.5–2 μm) secondary particles composed of nanosized (≤10 nm) LTO primary particles as the anode, combined with spherical $LiMn_2O_4$ particles [108]. This cell showed nearly

100 % capacity retention up to 1000 cycles when cycled at 5*C* rate at 55 °C. However, the problem with the use of $LiMn_2O_4$ is not the cycling life (number of cycles before aging), but the calendar life, which is very limited by the dissolution of manganese in the electrolyte. In addition, as any chemical process, the kinetics of this dissolution process increases with temperature. An illustration of this effect was given by the failure of $LiMn_2O_4$-based batteries that equipped electric cars in the US after a hot summer in 2013, which forced the car-maker to recall these cars to change the batteries. That is why many efforts were made since 10 years to replace $LiMn_2O_4$ by a compound based on another transition metal that does not dissolve into the electrolyte. The LTO//$LiFePO_4$ (LFP) cell operates at voltage circa 1.75 V and has been first studied in 1994, using a gel-polymer electrolyte [109]. A liquid electrolyte made of Li salt in an ionic liquid, namely, lithiumbis(trifluoromethane) sulfonamide, LiTFSI in Py_{24}TFSI, is also viable [110]. When the $LiFePO_4$ particles used as cathode of the LTO//LFP cell are coated with a conductive layer to increase the electrical conductivity of the LFP powder, the cell delivers a capacity of 155 mAh g^{-1}. In one case, the coat was polyacene [111], but usually it is simply a 2–3 nm thick conductive carbon layer [112]. A breakthrough performance has been obtained with such carbon-coated nano-LFP (particle size, 25 nm) as cathode [96]. The cells retained full capacity after 20000 cycles performed at charge rate of 10*C* and discharge rate of 5*C*, and retained 95 % of the capacity after 30000 cycles at charge rate 15*C* and discharge rate 5*C*, both at 100 % DOD (depth of discharge) and 100 % SOC (state of charge). The performance has even been improved by using carbon-coated LTO particles of size 90 nm, as good rate capability has been observed up to 100*C* rate [113]. In addition, different electrolytes have been tested in this work in order to increase the temperature where the battery can operate, which imposes to get rid of the ethylene carbonate that has a too small boiling temperature. The upper bound of the temperature window where the "18650" battery operates is raised to 80 °C by using 1 mol L^{-1} lithium bis (fluorosulfonyl)imide (LiFSI) in GBL or 1 mol L^{-1} LiFSI in PC+ γ-butyrolactone (GBL) electrolyte. Studies have also been successful to decrease the lower limit of the temperature window. The "18650" cell using the low temperature electrolyte 1 mol L^{-1} $LiPF_6$ and 0.2 mol L^{-1} LiFSI in quaternary blend of aliphatic solvents such as propylene (PC) + methyl propionate (MP) + ethylmethyl carbonate (EMC) + 5 % fluorinated ethylene carbonate (FEC) (1:1:1:1 by volume) displayed a similar electrochemical performance at 25 °C as that of the cell with conventional electrolyte, but in contrast permits to pass the Hybrid pulse power characterization (HPPC) test down to −10 °C, owing to improvement in ionic conductivity of the electrolyte. In addition, accelerated rate calorimetry measurements have shown that this cell benefits from an unprecedented safety [113]. The LTO/LFP combination then appears as the most attractive battery for use in PHEV, and energy storage for wind and solar energy. As mentioned earlier, the $LiNi_{1/2}Mn_{3/2}O_4$ (LNM) cathode, which operates at 4.7 V with respect to Li, cannot be combined with graphite, and LTO has then been considered as an alternative anode by the Ohzuku group [104, 114, 115]. The LNM//LTO cell operates at 3.2 V and delivers a capacity decreasing from 5.4− 4.8 mAh (for mass balanced cells of 0.056 g LTO and 0.049 g LNM)

when the current rate increases from 12.7 to 509 mA g^{-1}. The Amine group found a 86 % capacity retention when the LNM//LTO cell was cycled at *C*-rates from 0.5 to 10*C*, with very good cyclability over 1000 cycles between 2.0 and 3.5 V [116]. A Li$(Ni_{0.45}Co_{0.1}Mn_{1.45})O_4$//LTO with weight ratio of anode to cathode 1.36 in the laminated-type cell delivered a capacity of 124 mAh g^{1} up to 500 cycles at 1*C* rate [117]. Let us recall, however, that the problem with LNM (Co-doped or not) is the dissolution of manganese in the conventional electrolytes (same problem as in the case of the $LiMn_2O_4$) that reduces the calendar life and is still an obstacle to the commercialization of such batteries.

LTO has also been combined with the layered oxides $LiCoO_2$ [102], $Li(Ni_{0.8}Co_{0.2})O_2$, $Li(Co_{1/2}Ni_{1/2})O_2$ [118], $Li(Co_{1/3}Ni_{1/3}Mn_{1/3})O_2$ [104], and $Li_{1+x}[Co_{1/3}Ni_{1/3}Mn_{1/3}]_{1-x}O_2$ [119]. The performance of such batteries is good. The interest in the use of such layered compounds as cathodes is the high energy density. For instance, LTO//$Li(Co_{1/3}Ni_{1/3}Mn_{1/3})O_2$ cell delivered a capacity $<$85 mAh g^{-1} (340 mAh cm^{-3}) and has an energy density of 215 Wh kg^{-1} or 970 Wh dm^{-3} with an average voltage of 2.5 V. The replacement of graphite by LTO improves the power of the battery, since this material does not change volume upon insertion of lithium, and supports much faster charge–discharge rates than graphite. The safety problem with layer compounds, however, remains. Their bad thermal stability has restricted the use of these materials as cathode of LiBs to applications to portable use, with the exception of Boeing and Tesla, who used Al-doped $Li(Ni_{0.8}Co_{0.2})O_2$//graphite, inevitably leading to the battery fires that they have experienced if the BMS cannot manage the intrinsic instability of these batteries. That is why we did not recommend their use in transportation in spite of the temptation of the higher energy density.

Other batteries have been studied at the laboratory scale, using other compounds that are extensively reviewed in Chap. 10 as promising anode elements. They are, however, still too far from commercial use to be listed in Table 2.7. In addition, as we see in Chap. 10, the performance of these materials depend very much on the composition of the anode electrodes, and the research today is focused on their optimization by working on the formation of composites associating for instance carbon under the form of nanotubes or graphene, or coat of the nanoparticles of active elements of different shape (spherical, nanotubes, nanoplates), and different porosity. A review of primary results on such full cells (by opposition to half-cells with Li as the anode studied in Chap. 10) can be found for instance in ref. [120], but they will be fast outdated by the progress on the building of the anodes and the results newly obtained on half-cells discussed in Chap. 10, owing to the progress in nanoscience and materials science.

2.4.2.3 Design and Manufacturing

The elementary electrochemical cell of the lithium-ion battery is based on the assembly of three main components. This cell comprises two reversible electrodes that are slurry deposited onto metallic current collector: the anode provides lithium

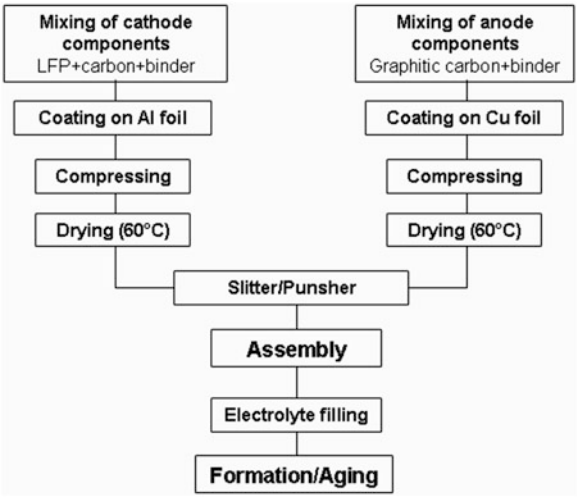

Fig. 2.9 Chart of manufacturing a Li-ion battery

ions during discharge and the cathode receives these charge species which are inserted into its lattice. The two electrodes are separated by a porous membrane with foam structure (separator) [121] soaked with the liquid electrolyte. This electrolyte is a fast ion conductor of lithium ions, but it is also an electronic insulator, because any transport of electron across the electrolyte would result in a self-discharge. The ionic conductivity is achieved by dissolving lithium salts in aprotic solvents. The anode is deposited onto copper foil, while the cathode material that is a mixture of electro-active material, carbon black and binder, is coated onto an aluminum foil. Both metallic foils insure the function of current collector. Each electrode film spread by coating technique has a thickness of a few tens of microns and a width of a few centimeters. Numerous operations are made to construct a cell, from preparation of powders and coating to cell formation and electrical tests (Fig. 2.9). The total thickness of the laminate obtained is about 150 μm, which depends on the electrical characteristics of the required cell. Indeed, changing the film thickness maximizes performance to meet the specific request of the application. So assemble thick film provides a configuration of high-energy type battery, while a thinner element will provide high-power performance. For a brief overview of processing for lithium-ion batteries see Ref. [122]. The sensitive chemistry of the Li-ion cell means that the manufacture must be done in dry room, less than 100 ppm of water. Mass production lies in fully automatic lines.

The manufacture of single cells and modules and packs for large-format power batteries is under development. One thing is inescapable: the manufacturing of cells in a dry room due to the sensitivity of lithium and chemistry to moisture. To satisfy the requirement of the target market of batteries for electric vehicles, the fabrication should be fast and less expensive, which necessitates fully automatic and integrated production lines. Such a solution has been adopted at Hydro-Québec, Canada, manufacturing 10-Ah iron-phosphate lithium-ion cells that are assembled in pack for power applications such as HEV, EVs and stationary storage.

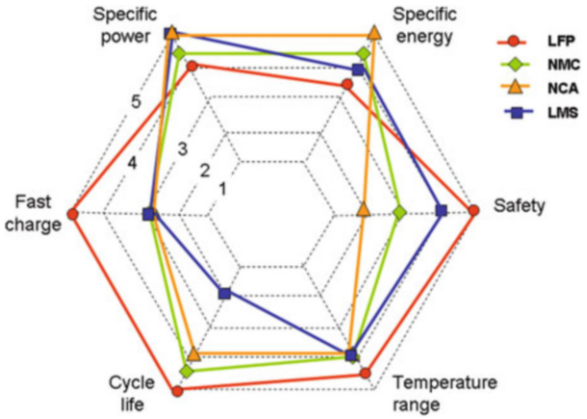

Fig. 2.10 Challenges in electrode materials for Li-ion batteries. *LFP* lithium iron phosphates. *NMC* nickel-manganese-cobalt oxide. *NCA* nickel-cobalt-aluminum oxide. *LMS* lithium-manganese spinel. Ranking: 1 = worst, 5 = best

Figure 2.10 compares the performance of various battery technologies envisaged for HEV and EV applications. Except energy and power density markers, the LFP chemistry shows the best characteristics in terms of fast charge, cycling, temperature runway and safety.

2.4.3 Lithium Polymer Batteries

In the 1980s Armand in collaboration with ELF-Aquitaine (France) and Hydro-Québec (Canada) played a leading role in the development of the lithium polymer battery (LMP) technology. Armand [123] suggested that solid polymer electrolytes derived from polyethylene oxide (PEO) might be used as electrolytes in LMP batteries, and major efforts have been made to produce polymer electrolytes with high conductivities at room temperature. Polymeric electrolytes are formed by complexes between salts of alkali metals and polymers containing solvating heteroatoms localized on the polymer chains. The most common example concerns such complexes with PEO chains that are formed by the repeat unit $–CH_2–CH_2–O–$. The solvating heteroatom, here oxygen, acts as a donor for the cation M^+. The anion X^-, generally of large dimension, stabilizes the PEO-M^+ complex. The first polymer electrolytes had conductivities of less than 10^{-5} S cm^{-1} at 25 °C, far too small for use in normal battery applications. Recently, however, electrolyte compositions have been produced which exhibit conductivity characteristics competitive with the properties of nonaqueous liquid electrolytes [124]. These materials have stimulated major development efforts in polymer electrolyte battery technology. The PEO-*MX* complexes may be considered as plastic electrolytes that are a compromise between liquid and solid crystalline electrolytes. Most of the polymeric batteries are of the form Li/PEO-Li salt/IC, where IC can be an intercalation compound, but also a composite electrode including a large amount of active intercalation material. From an examination of the temperature dependence of the ionic conductivity in polymer

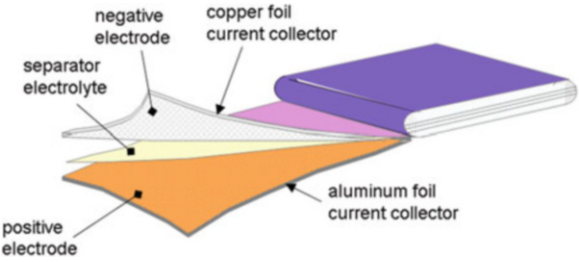

Fig. 2.11 Structure of a prismatic lithium-ion battery

complexes, one can remark the relatively high conductivity at room temperature of the complexes based on polyphosphazene, due to the low value of the vitreous transition temperature, T_g, and thus to the flexibility of the chains of the polymer, in turn related to the small barrier height to rotation of the P-N bond [125].

Positive electrodes of LPM batteries include a lithium-insertion electrode such as V_6O_{13}, TiS_2, MnO_2, Cr_3O_8, or LiV_3O_8 admixed with polymer electrolyte and conducting carbon for enhancement of the ionic and electronic conductivities, respectively. The composite electrode (50- to 75-μm thick) is deposited on a thin copper or nickel foil as current collector of few μm thick, and a film (25–50 μm) of $[(C_2H_4O)_9{\cdot}LiCF_3SO_3]_n$ polymer electrolyte completes the cell (Fig. 2.11). For optimum conductivity, the temperature of the polymer is maintained in the temperature range 80–90 °C. The system examined in the French–Canadian Project considered the following sequence $Li/(PEO)_8{\cdot}LiClO_4/TiS_2 + PEO + C$ [124]. Another system including TiO_2 as the cathode was cycled in the voltage range 3.0–1.2 V at a *C*/8 rate. A comparison of both cells shows similar features.

Recently, a LMP battery pack has been developed by Batscap that aims to demonstrate the feasibility of the high power LMP technology for EV application. It was especially designed to meet the needs for electric vehicles. This module, consisting of 12 cells connected in series is equipped with an electronic system (BMS) that provides thermal management (control of the internal temperature) and the electrical operation. The main information relating to security (alarm management) and the state of charge are managed and communicated to the application. With features in specific and volumetric energy density above 100 Wh kg^{-1} and 100 Wh L^{-1}, respectively, the 2.8-kWh BMP module (rated voltage 31 V) developed by BatScap realizes outstanding performance of lightness (25 kg) and compactness (25 L) and successfully equipped the fully electric Bluecar of the Bollore group.

2.4.4 Lithium-Sulfur Batteries

The lithium-sulfur (Li-S) battery has been under intense scrutiny for over two decades, as it offers the possibility of high gravimetric capacities and theoretical energy densities. Sulfur has a high specific capacity of 1673 mAh g^{-1}, but the rapid

capacity fading due to dissolution of polysulfides poses a significant challenge for practical applications. The discharge process of Li-S cell occurs with lithium dissolution from the anode surface and insertion into alkali-metal polysulfide salts, and reverse lithium plating to the anode while charging [126]. Theoretically, each sulfur atom can host two lithium ions, but experiments show that only 0.5–0.7 Li^+ ions are accommodated. Consequently, polysulfides are reduced while the cell is discharged according the reactions [126–129]:

$$S_8 \rightarrow Li_2S_8 \rightarrow Li_2S_6 \rightarrow Li_2S_4 \rightarrow Li_2S_3, \tag{2.19}$$

across a porous diffusion separator, sulfur polymers form at the cathode as the cell charges:

$$Li_2S \rightarrow Li_2S_2 \rightarrow Li_2S_3 \rightarrow Li_2S_4 \rightarrow Li_2S_6 \rightarrow Li_2S_8 \rightarrow S_8. \tag{2.20}$$

These reactions are analogous to those in the Na/S battery. Octasulfur has three forms: α-sulfur, β-sulfur, and γ-sulfur; the β-sulfur and γ-sulfur are metastable as they convert to α-sulfur in storage at ambient temperature. A typical discharge and charge voltage profile of the first cycle of Li//S cells is shown in Fig. 2.12.

Different configurations of Li//S batteries include silicon or lithium anode and a varieties of sulfur-based cathodes such as pure sulfur, porous TiO_2-encapsulated sulfur nanoparticles, sulfur-coated, disordered carbon nanotubes made from carbohydrates, copolymerized sulfur, sulfur-graphene oxide nanocomposite [129–132]. A 180-Å thick carbon layer was coated onto sulfur cathodes prepared by sputtering method. Charge–discharge tests show a specific capacity 1178 mAh g^{-1} at first discharge, falling to about 500 mAh g^{-1} after 50 cycles [132]. Ji et al. [130] reported the feasibility of a highly ordered nanostructured carbon-sulfur cathode for lithium-sulfur batteries. The conductive mesoporous carbon framework

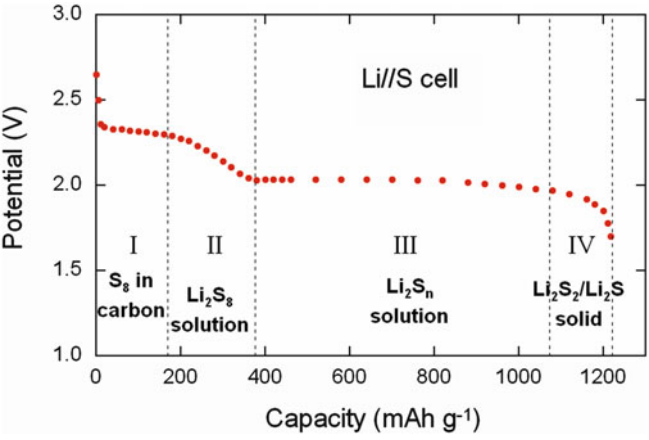

Fig. 2.12 Typical discharge and charge voltage profile of the first cycle of Li//S cells

precisely constrains sulfur nanofiller growth within its channels and generates essential electrical contact to the insulating sulfur. Such a structure favors access to Li reactivity with the sulfur. Reversible capacities up to 1320 mAh g^{-1} were attained. Zheng et al. [131] reported a hollow carbon nanofiber-encapsulated sulfur cathode for effective trapping of polysulfides, fabricated by using anodic aluminum oxide templates, and thermal carbonization of polystyrene. A high specific capacity of about 730 mAh g^{-1} was observed at *C*/5 rate after 150 cycles of charge–discharge. The introduction of $LiNO_3$ additive to the electrolyte was shown to improve the coulombic efficiency to over 99 % at rate *C*/5.

2.5 Economy of Lithium Batteries

Let us consider several aspects of lithium battery managements. Figure 2.13 displays some battery sizes including cylindrical, coin-cell, prismatic and pouch cell. A 2-Ah 18650 Li-ion cell has 0.6 g of lithium content. On a typical 60 Wh laptop battery with 8 cells (4 in series and 2 in parallel), this adds up to 4.8 g. To stay under the 8-g UN limit, the largest battery you can bring is 96 Wh. This pack could include 2.2 Ah cells in a 12 cells arrangement (4 series-3 parallels). If the 2.4-Ah cells were used instead, the pack would need to be limited to 9 cells (3 series-3 parallels). Evidently, the eventual commercial acceptability of lithium rechargeable batteries will depend on their cost effectiveness compared with other types of battery in the same utilization. In France, the cost of domestic electricity is 1.31€ per kWh including VAT and taxes (in January 2014); a AA-size alkaline Leclanché cell delivering, say 5 Wh, currently retails at 1.50€. Thus energy from this primary battery costs 300€/kWh, i.e., more expensive by a factor of over 200 with respect to the energy provided by domestic electricity.

Information from battery manufacturers are rather sparse but prices have now slipped to anywhere from $400 to $750 a kWh that means the 85-kWh pack powering the Tesla electric car costs between $34000 and $6375. A study by the Boston Consulting Group projected that prices would need to come down to

Fig. 2.13 Various battery configurations. (**a**) LS14250- cylindrical Li// $SOCl_2$ battery, (**b**) 4R25-prismatic (container) cell, (**c**–**d**) CR2020 Li-MnO_2 coin cells, (**e**) AA-type Li-ion cylindrical (1.5 Ah, 3.6 V, 12.4 g) cell, and (**f**) 30-Ah pouch ($LiMn_2O_4$-type, 3.8 V, 850 g) cell

$200 or less per kWh to make electric vehicles truly competitive. With a forecast of global demand of 26149 MWh by 2015, Sam Jaffe, research manager at IDC Corporate USA, claims a dramatic reduction in price for Li-ion cells to as low as $400/kWh [133]. Every year over 15 billion electrochemical cells are produced and sold worldwide including 40 % of lithium-based batteries. The global transportation lithium-ion battery market in light duty vehicles will grow from $1.6 billion in 2012 to almost $22 billion in 2020 with a nominal battery pack cost down to $397/kWh. According to Frost and Sullivan, in 2009, lithium battery market made up 40 % of the global revenue, overall 37 % of income for Li-ion batteries and 3 % for primary batteries. Presently, the greater part of general-use LiBs is produced in China, Japan, and the Republic of Korea. From statistics of calendar year 2013 provided by METI, the total battery production by volume was 3.46 billion units that produced a value 683.4 billion yens [134]. This production included 61 % primary batteries and 39 % secondary batteries (Fig. 2.2).

Battery recycling is a necessary issue to avoid hazardous waste and pollution especially when automobiles will be electrically powered. The process could be similar to that used for lead-acid batteries. Estimation made by Chemetall [135] show that recycling could provide 50 % of the lithium requirement for new batteries by 2040. Presently, it costs about $1700 to recycle 1 ton of batteries of any chemistry and size. From calculations by Hsiao and Richter [136], a 100-Ah battery processed through recycling would return 169 kg of Li carbonate, 38 kg of Co and 201 kg of Ni assuming the $LiNi_{0.8}Co_{0.15}Al_{0.05}O_2$ (NCA) cathode chemistry, for a total value of the recovered materials that exceeds $5000.

2.6 Battery Modeling

The constraints encountered by electrified automobiles, HEVs, PHEVs, and EVs, lead to very complex powertrain architectures, which require an optimized energy management obtained by simulation of the batteries. Battery modeling can help to predict, and possibly extend its lifetime. Many battery models can be found in the literature that are electrochemical models and stochastic models; for a review see Jongerden and Haverkort [137, 138]. The open-circuit voltage (thermodynamic property) is the main parameter taken into account in the electrochemical model, in which the charge transfer overvoltage, the diffusion overvoltage and the ohmic drop are considered (Eqs. 1.6 and 1.7). Due to various nonlinear effects the expression of the lifetime $t = Q/i$ does not hold for real battery, thus, a simple approximation for t under constant load i can be made with the Peukert' law (Eq. 1.26). The equivalent circuit used for simulation is obtained from experimental data of electrochemical impedance spectroscopy (EIS) of the battery at given state-of-charge [139].

Electrochemical properties and battery management of lithium metal and lithium-ion cells were analyzed using several different models. The electrochemical model developed by Doyle et al. [140–142] consists of six coupled, nonlinear differential equations whose solutions obtained from the Fortran program named

"Dualfoil" provide, with a very high accuracy, the voltage and current as functions of time and parameters of the battery electrolyte. Hageman has proposed the electrical-circuit models to evaluate Ni-Cd batteries [143]. A typical equivalent circuit includes five components: (1) a capacitor representing the capacity of the battery, (2) a discharge-rate normalizer that determines the lost capacity at high discharge currents, (3) a circuit to discharge the capacity of the battery, (4) a voltage versus state-of-charge lookup table, and (5) a resistor representing the battery's resistance. The Rakhmatov model is an extension of the Peukert's law based on the diffusion process of the active materials in the battery. To determine the lifetime one has to compute the diffusion process described by Fick's laws. This analytical model applied to Li-ion cells does even better, with a 2.7 % maximum error and an average error of less than 1 %.

In the kinetic battery model (KiBaM), Manwell and McGowan [144] used a chemical kinetics process with the battery charge distributed over two wells. For the calculation of the voltage during discharge, the battery is modeled as a voltage source in series with an internal resistance. The KiBaM can be used to model Li-phosphate-type Li-ion batteries because of the flat discharge profile of such a cell. The stochastic model based on discrete-time Markov chains was introduced by Chiasserini and Rao [145]. Modeling of Li-ion batteries has been obtained with a high accuracy, 1 % error. Later, in 2005, Rao et al. [146] proposed a stochastic battery model based on the analytical KiBaM. This simulation was successfully applied to AAA-type Ni-MH batteries with a maximum error of 2.65 %.

Tremblay and Dekkiche [147] presented an easy-to-use battery model applied to dynamic simulation software using the battery state-of-charge (SOC). Such a model is very similar to the Shepherd model that describes the electrochemical behavior of the battery directly in terms of voltage and current, often used in conjunction with the Peukert equation [148, 149]. However, contrary to the Shepherd model, it does not produce an algebraic loop. The battery is modeled using a simple controlled voltage source in series with a constant resistance, as shown in Fig. 1.7. This model assumes the same features for charge and discharge cycles. The open-voltage source is calculated with nonlinear Kalman filter that is an equation based on the actual SOC of the cell:

$$E = E_0 - K\frac{Q}{Q - it} + Ae^{\left(-B\int idt\right)}, \tag{2.21}$$

where E is the now-load voltage (V), E_0 the battery constant voltage (V), K the polarization voltage (V), Q the battery capacity (Ah), A the exponential zone amplitude (V), B the exponential zone time constant inverse $(\text{Ah})^{-1}$, and $\int idt$ the actual battery charge (Ah).

The long term calendar life of lithium ion cells for satellite and standby applications was studied by Broussely et al. [150]. In experiments, the capacity evolution was tracked as a function of storage temperature. Cells containing either $LiCoO_2$ or

$LiNi_xM_yO_2$ positive electrodes coupled with a graphite negative electrode were float-charged at 3.8 or 3.9 V. This study focused on losses at the negative electrode and the data were fit to a model involving a rate-determining step governed by electronic conductivity of the solid electrolyte interphase (SEI) layer, following Arrhenius law as a function of temperature.

References

1. Julien C, Nazri GA (1994) Solid state batteries: materials design and optimization. Kluwer, Boston
2. Goonan TG (2012) Lithium use in batteries. US Geological Survey Circular 1371, Reston, Virginia. http://pubs.usgs.gov/circ/1371/pdf/circ1371_508.pdf
3. Pistoia G (1994) Lithium batteries: new materials, developments and perspectives. Elsevier, Amsterdam
4. Linden D, Reddy TB (2001) Handbook of batteries, 3rd edn. McGraw-Hill, New York
5. Bergveld HJ, Kruijt WS, Notten PHL (2002) Battery management systems, design by modelling. Kluwer Academic Publishers, Dordrecht
6. Van Schalkwijk WA, Scrosati B (2002) Advances in lithium batteries. Kluwer, New York
7. Nazri GA, Pistoia G (2003) Lithium batteries, science and technology. Springer, New York
8. Balbuena PB, Wang Y (2004) Lithium-ion batteries, solid-electrolyte interphase. Imperial College Press, London
9. Wakihara M, Yamamoto O (2008) Lithium ion batteries: fundamentals and performance. Wiley, Weinheim
10. Yoshio M, Brodd RJ, Kozawa A (2009) Lithium batteries, science and technologies. Springer, New York
11. Ozawa K (2009) Lithium ion rechargeable batteries. Wiley, Weinheim
12. Park CR (ed) (2010) Lithium-ion batteries. InTech, Rijeka (Croatia) Open access book. http://www.intechopen.com/books/lithium-ion-batteries
13. Yuan X, Liu H, Jiujun Z (2012) Lithium batteries: advanced materials and technologies. CRC Press, Boca Raton
14. Belharouak I (ed) (2012) Lithium batteries new developments. InTech, Rijeka (Croatia) Open access book. http://www.intechopen.com/books/lithium-ion-batteries-new-developments
15. Abu-Lebdeh Y, Davidson I (2013) Nanotechnology for lithium-ion batteries. Springer, New York
16. Scrosati B, Abraham KM, Van Schalkwijk WA, Hassoun J (2013) Lithium batteries: advanced technologies and applications. Wiley, Hoboken
17. Jasinski R (1967) High-energy batteries. Plenum, New York
18. Julien C (2000) Design considerations for lithium batteries. In: Julien C, Stoynov Z (eds) Materials for lithium-ion batteries. Kluwer, Dordrecht, pp 1–20
19. Armand MB, Whittingham MS, Huggins RA (1972) The iron cyanide bronzes. Mater Res Bull 7:101–108
20. Armand MB (1973) Lithium intercalation in CrO_3 using n-butyllithium. In: Van Gool W (ed) Fast ion transport in solids. North Holland, Amsterdam, pp 665–673
21. Gamble FR, Osiecki JH, Cais M, Pisharody R, DiSalvo FL, Geballe TH (1971) Intercalation complexes of Lewis bases and layered sulfides: a large class of new superconductors. Science 174:493–497
22. Dines MB (1975) Intercalation of metallocenes in the layered transition-metal dichalcogenides. Science 188:1210–1211
23. Dines MB (1975) Lithium intercalation via n-butyllithium of the layered transition metal dichalcogenides. Mater Res Bull 10:287–292

24. Whittingham MS (1978) Chemistry of intercalation compounds: metal guests in chalcogenaide hosts. Prog Solid State Chem 12:41–99
25. Whittingham MS (1982) Intercalation chemistry: an introduction. In: Whittingham MS, Jacobson AJ (eds) Intercalation chemistry. Academic, New York, pp 1–18
26. Winn DA, Steele BCH (1976) Thermodynamic characterization of non-stoichiometric titanium disulphide. Mater Res Bull 11:551–558
27. Winn DA, Shemilt JM, Steele BCH (1976) Titanium disulphide: a solid solution electrode for sodium and lithium. Mater Res Bull 11:559–566
28. Whittingham MS (1977) Preparation of stoichiometric titanium disulfide. US Patent 4,007,055, Accessed 8 Feb 1977
29. Murphy DW, Trumbore FA (1976) The chemistry of TiS_3 and $NbSe_3$ cathodes. J Electrochem Soc 123:960–964
30. Dickens PG, French SJ, Hight AT, Pye MF (1979) Phase relationships in the ambient temperature $Li_xV_2O_5$ system ($0.1 < x < 1.0$). Mater Res Bull 14:1295–1299
31. Toronto Globe and Mail (1989) Cellular phone recall may cause setback for Moli. Accessed 15 Aug 1989
32. Akridge JR, Vourlis H (1986) Solid state batteries using vitreous solid electrolytes. Solid State Ionics 18–19:1082–1087
33. Anderman M, Lunquist JT, Johnson SL, Gionannoi TR (1989) Rechargeable lithium-titanium disulphide cells of spirally-wound design. J Power Sourc 26:309–312
34. Abraham KM, Pasquariello DM, Schwartz DA (1989) Practical rechargeable lithium batteries. J Power Sourc 26:247–255
35. Armand M (1980) Intercalation electrodes. In: Murphy DW, Broadhead J, Steele BCH (eds) Materials for advanced batteries. Plenum Press, New York, pp 145–161
36. Lazzari M, Scrosati B (1980) A cycleable lithium organic electrolyte cell based on two intercalation electrodes. J Electrochem Soc 127:773–774
37. Nagaura T, Nagamine M, Tanabe I, Miyamoto N (1989) Solid state batteries with sulfide-based solid electrolytes. Prog Batteries Sol Cells 8:84–88
38. Nagaura T, Tozawa K (1990) Lithium ion rechargeable battery. Prog Batteries Solar Cells 9:209–212
39. Goodenough JB, Mizuchima K (1981) Electrochemical cell with new fast ion conductors. US Patent 4,302,518, Accessed 24 Nov 1981
40. Mizushima K, Jones PC, Wiseman PJ, Goodenough JB (1980) Li_xCoO_2 ($0 < x < 1$): a new cathode material for batteries of high energy density. Mater Res Bull 15:783–789
41. Armand M, Touzain P (1977) Graphite intercalation compounds as cathode materials. Mater Sci Eng 31:319–329
42. Ozawa K (1994) Lithium-ion rechargeable batteries with $LiCoO_2$ and carbon electrodes: the $LiCoO_2$/C system. Solid State Ionics 69:212–221
43. Frost & Sullivan (2013) Global lithium-ion market to double despite recent issues. http://www.frost.com. Accessed 21 Feb 2013
44. Freedonia (2013) Batteries, study ID 3075. http://www.freedoniagroup.com/industry-category/enrg/energy-and-power-equipment.htm. Accessed Nov 2013
45. Julien C (1997) Solid state batteries. In: Gellings PJ, Bouwmeester HJM (eds) The CRC handbook of solid state electrochemistry. CRC Press, Boca Raton, pp 372–406
46. Ritchie AG, Bowles PG, Scattergood DP (2004) Lithium-iron/iron sulphide rechargeable batteries. J Power Sourc 136:276–280
47. Jensen J (1980) Energy storage. Butterworths, London
48. Holmes CF (2007) The lithium/iodine-polyvinylpyridine battery – 35 years of successful clinical use. ECS Trans 6:1–7
49. Mallela VS, Ilankumaran V, Rao NS (2004) Trends in cardiac pacemaker batteries. Indian Pacing Electrophysiol J 4:201–212
50. Schlaikjer CR, Liang CC (1971) Ionic conduction in calcium doped polycrystalline lithium iodide. J Electrochem Soc 118:1447–1450

51. Phillips GM, Untereker DF (1980) In: Owens BB, Margalit N (eds) Power sources for biomedical implantable applications and ambient temperature lithium batteries. The Electrochem Soc Proc Ser PV 870-4, p 195
52. Liang CC, Joshi AV, Hamilton WE (1978) Solid-state storage batteries. J Appl Electrochem 8:445–454
53. Park KH, Miles MH, Bliss DE, Stilwell D, Hollins RA, Rhein RA (1988) The discharge behaviour of active metal anodes in bromine trifluoride. J Electrochem Soc 135:2901–2902
54. Goodson FR, Shipman WH, McCartney JF (1978) Lithium anode, bromide trifluoride, antimony pentafluoride. US Patent 4,107,401 A, Accessed 15 Aug 1978
55. Crepy G, Buchel JP (1993) Lithium/bromide trifluoride electrochemical cell designed to be discharged after being activated and stored. US Patent 5,188,913 A, Accessed 23 Feb 1993
56. Bowden WL, Dey AN (1980) Primary Li/$SOCl_2$ cells XI. $SOCl_2$ reduction mechanism in a supporting electrolyte. J Electrochem Soc 127:1419–1426
57. Dey AN, Holmes RW (1980) Safety studies on Li/SO_2 cells: investigations of alternative organic electrolytes for improved safety. J Electrochem Soc 127:1886–1890
58. PowerStream (2014) Primary lithium SO_2 cells from PowerStream http://www.powerstream.com/LiPSO2.htm
59. Leising RA, Takeuchi ES (1993) Solid-state cathode materials for lithium batteries: effect of synthesis temperature on the physical and electrochemical properties of silver vanadium oxide. Chem Mater 5:738–742
60. Holmes CF (2001) The role of lithium batteries in modern health care. J Power Sourc 97–98:739–741
61. Root MJ (2010) Lithium-manganese dioxide cells for implantable defibrillator devices, discharge voltage models. J Power Sourc 195:5089–5093
62. Chen K, Meritt DR, Howard WG, Schmidt CL, Skarstad PM (2006) Hybrid cathode lithium batteries for implantable medical applications. J Power Sourc 162:837–840
63. Walk CR (1983) Lithium-vanadium pentoxide cells. In: Gabano JP (ed) Lithium batteries. Academic, London, pp 265–280
64. Whittingham MS (1975) Mechanism of reduction of the fluorographite cathode. J Electrochem Soc 122:526–527
65. Touhara H, Kadono K, Fujii Y, Watanabe N (1987) On the structure of graphite fluoride. Z Anorg Allg Chem 544:7–20
66. Lam P, Yazami R (2006) Physical characteristics and rate performance of $(CF_x)_n$ $(0.33 < x < 0.66)$ in lithium batteries. J Power Sourc 153:354–359
67. Nagasubramanian G (2007) Fabrication and testing capabilities for 18650 Li/$(CF_x)_n$ cells. Int J Electrochem Sci 2:913–922
68. Holmes CF, Takeuchi ES, Ebel SJ (1996) Lithium/carbon monofluoride (Li//CF_x): a new pacemaker battery. Pacing Clin Electrophys 19:1836–1840
69. Shmuel De-Leon (2011) Li/CFx batteries the renaissance. http://www.sdle.co.il/AllSites/810/Assets/li-cfx%20-%20the%20renaissance.pdf. Accessed 8 June 2011
70. Broussely M (1978) Organic solvent electrolytes for high specific energy primary cells. US Patent 4,129,691A, Accessed 12 Dec 1978
71. Webber A (2009) Low temperature Li/FeS_2 battery. US paten 7,510,808B2, Accessed 31 Mar 2009
72. Clark MB (1982) Lithium-iron disulfide cells. Academic, New York
73. Shao-Horn Y, Osmialowski S, Horn QC (2002) Nano-FeS_2 for commercial Li/FeS_2 primary batteries. J Electrochem Soc 149:A1199–A1502
74. West K, Crespi AM (1995) Lithium insertion into silver vanadium oxide $Ag_2V_4O_{11}$. J Power Sourc 54:334–337
75. Crespi AM (1993) Silver vanadium oxide cathode material and method of preparation. US Patent 5,221,453, Accessed 27 Sept 1990
76. Crespi A, Schmildt C, Norton J, Chen K, Skarstad P (2001) Modeling and characterization of the resistance of lithium/SVO for implantable cardioverter-defibrillators. J Electrochem Soc 148:A30–A37

77. Chung JS, Sohn HJ (2002) Electrochemical behaviours of CuS as a cathode material for lithium secondary batteries. J Power Sourc 108:226–231
78. Whittingham MS (2004) Lithium batteries and cathode materials. Chem Rev 104:4271–4301
79. Rao BML, Francis RW, Christopher HA (1977) Lithium-aluminum electrode. J Electrochem Soc 124:1490–1492
80. Xu K (2004) Nonaqueous liquid electrolytes for lithium-based rechargeable batteries. Chem Rev 104:4303–4417
81. Ota H (2004) Characterization of lithium electrodes in lithium imides/ethylene carbonate and cyclic ether electrolytes. Surface chemistry. J Electrochem Soc 151:A437–A446
82. Von Sacken U, Nodwell E, Sundher A, Dahn JR (1990) Comparative thermal stability of carbon intercalation anodes and lithium metal anodes for rechargeable lithium batteries. J Power Sourc 54:240–245
83. Whittingham MS (1978) The electrochemical characteristics of VSe_2 in lithium cells. Mater Res Bul 13:959–965
84. Akridge JR, Vourlis H (1988) Performance of Li/TiS_2 solid state batteries using phosphorous chacogenide network former glasses as solid electrolyte. Solid State Ionics 28–30:841–846
85. Py MA, Haering RR (1983) Structural destabilization induced by lithium intercalation in MoS_2 and related compounds. Can J Phys 61:76–84
86. Trumbore FA (1989) Niobium triselenide: a unique rechargeable positive electrode material. J Power Sourc 26:65–75
87. Schöllhorn R, Kuhlmann R, Besenhard JO (1976) Topotactic redox reactions and ion exchange of layered MoO_3 bronzes. Mater Res Bull 11:83–90
88. Besenhard JO, Schöllhorn R (1976) The discharge reaction mechanism of the MoO_3 electrode in organic electrolytes. J Power Sourc 1:267–276
89. Murphy DW, Christian PA, DiSalvo FJ, Waszczak JV (1979) Lithium incorporation by vanadium pentoxide. Inorg Chem 18:2800–2803
90. Labat J, Cocciantelli JM (1990) Rechargeable electrochemical cell having a cathode based on vanadium oxide. US Patent No. 5,219,677, Accessed 11 Dec 1990
91. Margalit N, Walk CR (1995) Lithium ion battery with lithium vanadium pentoxide positive electrode. World Patent WO 1996006465 A1, Accessed 18 Aug 1995
92. Desilvestro J, Haas O (1990) Metal oxide cathode materials for electrochemical energy storage. J Electrochem Soc 137:5C–22C
93. Zaghib K, Mauger A, Groult H, Goodenough JB, Julien CM (2013) Advanced electrodes for high power Li-ion batteries. Materials 6:1028–1049
94. Julien CM, Mauger A, Zaghib K, Groult H (2014) Comparative issues of cathode materials for Li-ion batteries. Inorganics 2:132–154
95. Zaghib K, Guerfi A, Hovington P, Vijh A, Trudeau M, Mauger A, Goodenough JB, Julien CM (2013) Review and analysis of nanostructured olivine-based lithium rechargeable batteries: status and trends. J Power Sourc 232:357–369
96. Zaghib K, Dontigny M, Guerfi A, Charest P, Rodrigues I, Mauger A, Julien CM (2011) Safe and fast-charging Li-ion battery with long shelf life for power applications. J Power Sourc 196:3949–3954
97. Goodenough JB, Kim Y (2010) Challenges for rechargeable Li batteries. Chem Mat 22:587–603
98. Peled E (1979) The electrochemical behaviour of alkali and alkaline earth metals in nonaqueous battery systems. The solid electrolyte interphase model. J Electrochem Soc 126:2047–2051
99. Aurbach D, Gamolsky K, Markovsky B, Salitra G, Gofer Y, Heider U, Oesten R, Schmidt M (2000) The study of surface phenomena related to electrochemical lithium intercalation into Li_xMO_y host materials (M = Ni, Mn). J Electrochem Soc 147:1322–1331
100. Ferg E, Gummow RJ, Dekock A, Thackeray MM (1994) Spinel anodes for lithium-ion batteries. J Electrochem Soc 141:L147–L150

101. Peramunage D, Abraham KM (1998) Preparation of micron-sized $Li_4Ti_5O_{12}$ and its electrochemistry in polyacrylonitrile electrolyte-based lithium cells. J Electrochem Soc 145:2609–2615
102. Jansen AN, Kahaian AJ, Kepler KD, Nelson PA, Amine K, Dees DW, Vissers DR, Thackeray MM (1999) Development of a high-power lithium-ion battery. J Power Sourc 81:902–905
103. Ohzuku T, Yamato R, Kawai T, Ariyoshi K (2008) Steady-state polarization measurements of lithium insertion electrodes for high-power lithium-ion batteries. J Solid State Electrochem 128:979–985
104. Ariyoshi K, Ohzuku T (2007) Conceptual design for 12 V "lead-free" accumulators for automobile and stationary applications. J Power Sourc 174:1258–1262
105. Lu W, Belharouak I, Liu J, Amine K (2007) Thermal properties of $Li_{4/3}Ti_{5/3}O_4/LiMn_2O_4$ cell. J Power Sourc 174:673–677
106. Belharouak I, Sun YK, Lu W, Amine K (2007) On the safety of the $Li_4Ti_5O_{12}$ /$LiMn_2O_4$ lithium-ion battery system batteries and energy storage. J Electrochem Soc 154:A1083–A1087
107. Du Pasquier A, Huang CC, Spitler T (2009) Nano $Li_4Ti_5O_{12}$-$LiMn_2O_4$ batteries with high power capability and improved cycle-life. J Power Sourc 186:508–514
108. Amine K, Belharouak I, Chen ZH, Tran T, Yumoto H, Ota N, Myung ST, Sun YK (2010) Nanostructured anode material for high-power battery system in electric vehicles. Adv Mater 22:3052–3057
109. Reale P, Panero S, Scrosati B, Garche J, Wohlfahrt-Mehrens M, Wachtler M (2004) A safe, low-cost, and sustainable lithium-ion polymer battery. J Electrochem Soc 151:A2138–A2142
110. Reale P, Fernicola A, Scrosati B (2009) Compatibility of the Py_{24}TFSI-LiTFSI ionic liquid solution with $Li_4Ti_5O_{12}$ and $LiFePO_4$ lithium ion battery electrodes. J Power Sourc 194:182–189
111. Sun LQ, Cui RH, Jalbout AF, Li MJ, Pan XM, Wang RS, Xie HM (2009) $LiFePO_4$ as an optimum power cell material. J Power Sourc 189:522–526
112. Jaiswal A, Horne CR, Chang O, Zhang W, Kong W, Wang E, Chern T, Doeff MM (2009) Nanoscale $LiFePO_4$ and $Li_4Ti_5O_{12}$ for high rate Li-ion batteries and energy storage. J Electrochem Soc 156:A1041–A1046
113. Zaghib K, Dontigny M, Guerfi A, Trottier J, Hamel-Paquet J, Gariepy V, Galoutov K, Hovington P, Mauger A, Julien CM (2012) An improved high-power battery with increased thermal operating range: C-$LiFePO_4$//C-$Li_4Ti_5O_{12}$. J Power Sourc 216:192–200
114. Ohzuku T, Ariyoshi K, Yamamoto S, Makimura Y (2001) A 3-volt lithium-ion cell with Li$[Ni_{1/2}Mn_{3/2}]O_4$ and Li$[Li_{1/3}Ti_{5/3}]O_4$: a method to prepare stable positive-electrode material of highly crystallized Li$[Ni_{1/2}Mn_{3/2}]O_4$. Chem Lett 1270–1271
115. Ariyoshi K, Yamamoto S, Ohzuku T (2003) Three-volt lithium-ion battery with Li$[Ni_{1/2}Mn_{3/2}]O_4$ and the zero-strain insertion material of Li$[Li_{1/3}Ti_{5/3}]O_4$. J Power Sourc 119:959–963
116. Wu HM, Belharouak I, Deng H, Abouimrane A, Sun YK, Amine K (2009) Development of $LiNi_{0.5}Mn_{1.5}O_4/Li_4Ti_5O_{12}$ system with long cycle life batteries and energy storage. J Electrochem Soc 156:A1047–A1050
117. Jung HG, Jang MW, Hassoun J, Sun YK, Scrosati B (2011) A high-rate long-life $Li_4Ti_5O_{12}$/Li$[Ni_{0.45}Co_{0.1}Mn_{1.45}]O_4$ lithium-ion battery. Nat Commun 2:516
118. Sawai K, Yamato R, Ohzuku T (2006) Impedance measurements on lithium-ion battery consisting of Li$[Li_{1/3}Ti_{5/3}]O_4$ and Li$(Co_{1/2}Ni_{1/2})O_2$. Electrochim Acta 51:1651–1655
119. Lu W, Liu J, Sun YK, Amine K (2007) Electrochemical performance of $Li_{4/3}Ti_{5/3}O_4/Li_{1+x}(Ni_{1/3}Co_{1/3}Mn_{1/3})_{1-x}O_2$ cell for high power applications. J Power Sourc 167:212–216
120. Reddy MV, Suba Rao GV, Chowdari BVR (2013) Metal oxides and oxysalts as anode materials for Li ion batteries. Chem Rev 113:5364–5457
121. Arora P, Zhang Z (2004) Battery separators. Chem Rev 104:4419–4462
122. Daniel C (2008) Materials and processing for lithium-ion batteries. JOM 60:43–48
123. Armand MB (1983) Polymer solid electrolytes – an overview. Solid State Ionics 9–10:745–754

124. Gauthier M, Fauteux D, Vassort G, Belanger A, Duval M, Ricoux P, Gabano JP, Muller D, Rigaud P, Armand MB, Deroo D (1985) Assessment of polymer-electrolyte batteries for EV and ambient temperature applications. J Electrochem Soc 132:1333–1340
125. Armand M (1985) Ionically conductive polymers. In: Sequeira CAC, Hooper A (eds) Solid state batteries. Marinus Nijhoff, Dordrecht, pp 63–72
126. Zhang SS (2013) Liquid electrolyte lithium/sulfur battery: fundamental chemistry, problems, and solutions. J Power Sourc 231:153–162
127. Jeong SS, Lim Y, Choi YJ, Cho GB, Kim KW, Ahn HJ, Cho KK (2007) Electrochemical properties of lithium sulfur cells using PEO polymer electrolytes prepared under three different mixing conditions. J Power Sourc 174:745–750
128. Song MK, Zhang Y, Cairns EJ (2013) A long-life, high-rate lithium/sulfur cell: a multifaceted approach to enhancing cell performance. Nano Lett 13:5891–5899
129. Manthiram A, Fu Y, Su YS (2013) Challenges and prospects of lithium-sulfur batteries. Acc Chem Res 46:1125–1134
130. Ji X, Lee KT, Nazar LF (2009) A highly ordered nanostructured carbon-sulphur cathode for lithium-sulphur batteries. Nat Mater 8:500–506
131. Zheng G, Yang Y, Cha JJ, Hong SS, Cui Y (2011) Hollow carbon nanofiber-encapsulated sulfur cathodes for high specific capacity rechargeable lithium batteries. Nano Lett 11:4462–4467
132. Choi YJ, Ahn JH, Ahn HJ (2008) Effects of carbon coating on the electrochemical properties of sulfur cathode for lithium/sulfur cell. J Power Sourc 184:548–552
133. Jaffe S, Talon C, Ishimori K, Bigliani R, Tong F, Nicholson R (2001) Business strategy: lithium ion manufacturing global buildout, supply and demand forecasts. http://www.idc.com/getdoc.jsp?containerId=EI232266. Accessed Dec 2011
134. Battery Association of Japan (2014) Total battery production statistics. http://www.baj.or.jp/e/statistics/01.html
135. Chemetall (2009) Lithium applications and availability: Chemetall statement to investors, July 28. http://www.chemetall.com/fileadmin/files_chemetall/Downloads/Chemetall_Li-Supply_2009_July.pdf. Accessed 4 Jan 2009
136. Hsiao E, Richter C (2008) Electric vehicles special report – Lithium Nirvana – Powering the car of tomorrow. In: CLSA Asia-Pacific Markets. http://www.clsa.com/assets/files/reports/CLAS-Jp-ElectricVehicles20080530.pdf. Accessed 2 Dec 2009
137. Jongerden MR, Haverkort BR (2008) Which battery model to use? In: Dingle NJ, Haeder U, Argent-Katwala A (eds) UKPEW 2008. Imperial College, London, pp 76–88, http://doc.utwente.nl/64866/1/battery-model.pdf
138. Jongerden MR, Haverkort BR (2008) Battery modelling. Tech report TR-CIT-08-01. UTwente, Enschede. http://eprints.eemcs.utwente.nl/11645/01/BatteryRep4.pdf. Accessed 29 Jan 2008
139. Hafsaoui J, Scordia J, Sellier F, Aubret P (2012) Development of an electrochemical battery model and its parameters identification tool. Int J Automobile Eng 3:27–33
140. Doyle M, Fuller TF, Newman J (1993) Modeling of galvanostatic charge and discharge of the lithium/polymer/insertion cell. J Electrochem Soc 140:1526–1533
141. Fuller TF, Doyle M, Newman J (1994) Simulation and optimization of the dual lithium ion insertion cell. J Electrochem Soc 141:1–10
142. Fuller TF, Doyle M, Newman J (1994) Relaxation phenomena in lithium-ion-insertion cells. J Electrochem Soc 141:982–990
143. Hageman SC (1993) Simple PSpice models let you simulate common battery types. Electronic Design News 38:117–129
144. Manwell J, McGowan J (1993) Lead acid battery storage model for hybrid energy systems. Sol Energ 50:399–405
145. Chiasserini C, Rao R (2001) Energy efficient battery management. IEEE J Selected Areas Commun 19:1235–1245

146. Rao V, Singhal G, Kumar A, Navet N (2005) Battery model for embedded systems. In; Proceedings of the 18th international conference on VLSI design held jointly with 4th international conference on embedded systems design (VLSID'05) IEEE Computer Society, pp 105–110
147. Tremblay O, Dessaint LA, Dekkiche AI (2007) A generic battery model for the dynamic simulation of hybrid electric vehicles. In: Proceedings of the vehicle power and propulsion conference. Arlington, TX, IEEE, pp 284–289
148. Moore S, Merhdad E (1996) Texas A&M, an empirically based electrosource horizon lead-acid battery model, Strategies in Electric and Hybrid Vehicle Design, SAE J. SP-1156, paper 960448, pp 135–138
149. Unnewehr LE, Nasar SA (1982) Electric vehicle technology. Wiley, New York, pp 81–91
150. Broussely M, Herreyre S, Biensan P, Kasztejna P, Nechev K, Staniewicz RJ (2001) Aging mechanism in Li ion cells and calendar life predictions. J Power Sourc 97–98:13–21